manuscript

Vehicle Repositioning under Uncertainty

Qinshen Tang
Nanyang Business School, Nanyang Technological University, Singapore qinshen.tang@gmail.com

Yu Zhang
School of Business Administration, Southwestern University of Finance and Economics, China y.zhang@swufe.edu.cn

Minglong Zhou
Department of Analytics & Operations, National University of Singapore Business School, Singapore
minglong_zhou@u.nus.edu

We consider a general multi-period repositioning problem in vehicle-sharing networks such as bicycle-sharing systems, free-float car-sharing systems, and autonomous mobility-on-demand systems. This problem is subject to uncertainties along multiple dimensions—including demand, travel time, and repositioning duration—and faces several operational constraints such as the service level and cost budget. We propose a *robustness optimization* model to tackle these uncertainties; thus we aim to satisfy operational constraints under a reference distribution yet also to protect against ambiguity in the true distribution. This paper is the first, as far as we know, to incorporate various time-dependent uncertainties. We then reformulate the model and efficiently obtain solutions by solving a sequence of mixed-integer linear optimization problems. Extensive simulation studies demonstrate that our model yields remarkable performance in various settings and is computationally scalable. We find that our model, when compared to such benchmarks as "fluid-based optimization", achieves the highest average service level for a given repositioning cost budget; it also is robust to adverse circumstances (i.e., its worst-case service level is also the highest).

Key words: vehicle repositioning; vehicle-sharing; uncertain travel time; uncertain repositioning duration

1. Introduction

The vehicle-sharing market has grown significantly over the past few years—encouraged by a "sharing" economy and development of the autonomous vehicle industry—and has been popularized by the younger, more environmentally conscious generation, and by the notion of urban mobility. A typical vehicle-sharing network consists of an operator, a fixed number of vehicles, and a service region with some service locations. These service locations could be rental stores or docks in station-based systems, or "subregions" in free-float systems. The operator serves customers in the region over a fixed operating horizon. During each period, customers arrive at different locations and pick up vehicles if available; then they travel to their destinations. The most common vehicle-sharing networks include, among many others, bike-sharing systems (e.g., Citi Bike in New York City and BLUEbikes in Boston) and free-float car-sharing platforms (e.g., Car2Go and Zipcar).

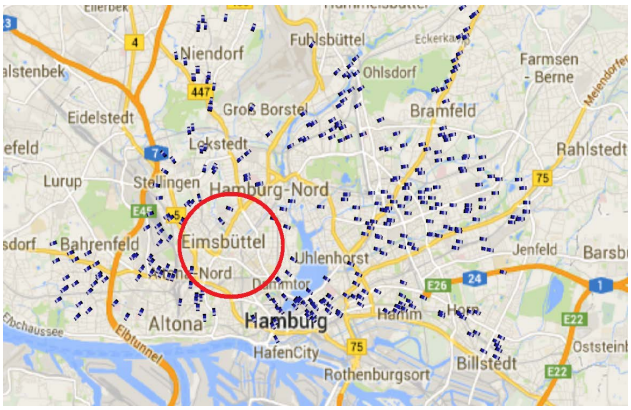

Figure 1 Screenshot showing the cars available in the Car2Go vehicle-sharing system in Hamburg (Herrmann et al. 2014)

A similar network structure is evident also in container deployment problems (Crainic et al. 1993), product rental networks (Benjaafar et al. 2017), and autonomous mobility-on-demand systems (Pavone 2015).

Demand and supply of vehicles are easily unbalanced in vehicle-sharing systems. For instance, the real-world case of Hamburg's Car2Go system at 9 AM on a work day, is depicted in Figure 1. We can see that there are only three cars in the red circled area (whose diameter is 3 km), which means that a potential customer in that area will be hard pressed to find a vehicle. As articulated in Ghosh et al. (2017), the unbalanced usage of vehicles in a sharing system leads either to congestion or to an insufficient stock of conveyances at locations each day. Traffic congestion is responsible for an annual loss, estimated as ranging between 2% to 5%, in the GDP of Asian economics (Kabra et al. 2018). An imbalance between demand and supply directly results in an appreciable amount of unmet demand. According to Serna et al. (2017), 16.4% of demand could be lost because of system unavailability due to the uneven usage and distribution of vehicles. To mitigate this imbalance, operators, in practice, usually periodically review the number of available vehicles at each location and reposition them among different locations. In addition, the loss from underserved demand is one of an operator's largest operational costs (Freund et al. 2018). It follows that the management of repositioning activities—that is, to help balance demand and supply and thereby increase system availability—is crucial to the successful implementation of a vehicle-sharing system (The Economist 2011). However, such systems are typically complicated by the large number of vehicles that must be repositioned simultaneously among hundreds of locations (Li et al. 2018). The optimization of these repositioning activities is, indeed, a most complex and challenging task.

One of the main difficulties in balancing demand and supply in vehicle-sharing networks arises from the stochastic nature of such systems. In the first place, system demand is uncertain; that is, the number of customers arriving at each location over the operating horizon is not known to the

operator beforehand. Also, customer travel destinations and travel times are uncertain. Finally, the time required to reposition a vehicle from one location to another—what we refer to as the *repositioning duration*—is likewise uncertain and is subject to time-varying traffic conditions.

Another difficulty is the operator—when making repositioning decisions—must satisfy a set of practical constraints, such as service-level targets and repositioning cost budget. For instance, Citi Bike is run by Motivate (a private company) under service-level agreements with the New York City Department of Transportation (Banerjee et al. 2016). Some operators (e.g., Vélib' in Paris) are even penalized by the local government when demand is being poorly served (Schuijbroek et al. 2017). It is also plausible for the operator to limit the total cost within a budget, especially when such systems are managed by non-profit organizations (e.g., Pronto in Seattle). Many of such constraints are subject to uncertainties; therefore, these constraints may not be strict. Instead, the operator may want to satisfy them as much as possible under uncertainties. When these uncertainties are misspecified, however, operational constraints can easily be violated in practice. Traditional approaches that consider only expectations fail to capture either how often the problem is infeasible and how severe that infeasibility can be. And since data are usually limited, the sample average may deviate significantly from the true expected value.

These difficulties make the vehicle repositioning problem that we consider involve four significant challenges. First, time-varying and spatially-unbalanced travel patterns require that vehicles be repositioned so as to ensure vehicle availability at most locations (He et al. 2019). The operator must allocate capacity between real-time demands and forecasted future demands. This balance is usually achieved by analyzing and solving dynamic programming problems. However, dynamic programming suffers from the "curse of dimensionality": computational complexity grows exponentially with the number of locations and planning periods. Second, customer travel patterns and adoption behaviors are highly uncertain at the planning stage (He et al. 2019). The firm will seldom have data that accurately characterize all the uncertainties *before* it makes some operational decisions. Third, it is difficult to identify the optimal repositioning decisions because such decisions have a long-term and global effect, and neither is it clear whether they will result in better system performance (Li et al. 2018). Fourth, it is not obvious how the operational constraints should be addressed. It is hard to derive reliable estimates of the monetary costs of violating different operational constraints and define the monetary trade-offs among multiple performance criteria. Hence, cost-driven optimization frameworks, which have been widely adopted, suffer from inaccurate cost parameters. Altogether, these considerations make it difficult to build a model that is both tractable and practical.

We shall address these challenges by focusing on the three questions. How can uncertainties be modeled so that they properly reflect real-world dynamics? How can we devise a practical model

while maintaining computational tractability? And perhaps more importantly: How can effective repositioning decisions be made so that, under uncertainty, operational constraints can be satisfied to the greatest extent possible?

We adopt a *robustness optimization* (RnO) paradigm (motivated by Jaillet et al. 2016 and Long et al. 2019) to satisfy operational constraints as much as possible in a multi-period vehicle repositioning problem under various time-dependent uncertainties. The robustness optimization framework is an alternative modeling paradigm for addressing optimization under uncertainty that aims to maximize the robustness of operational constraints. It seeks to satisfy (as much as possible) operational constraints under a reference distribution and also to protect against ambiguity in true distribution at a given cost budget. Using a novel construction of the vehicle-sharing network (as inspired by Bandi and Loke 2018), we show that the system dynamics can be modeled under a robustness optimization framework tractably. In this model, the operator must prescribe a cost budget and a set of operational constraints. These are practically relevant objectives because the operator usually has specific operational targets to achieve. We show that solutions to the RnO model can easily be derived by solving a sequence of mixed-integer linear optimization (MILO) problems. Next, we conduct extensive numerical experiments in which our model is implemented in a rolling horizon manner. This computational study reveals that our model outperforms such benchmarks as the deterministic model and the fluid-based optimization model of Braverman et al. (2019). In addition, the RnO model is computationally efficient.

Our four principal contributions to the literature can be summarized as follows.

1. We model the repositioning problem in vehicle-sharing systems under a robustness optimization framework, which is different from traditional models used in this context. Our model aims to satisfy, as much as possible, operational constraints under various real-world uncertainties. It also circumvents the need for an accurate stipulation of the monetary trade-offs among operational constraints such as service level and cost budget.

2. By a novel construction, we model the system dynamics of the vehicle-sharing network in a tractable way. Thus we efficiently obtain solutions from the RnO model by solving a sequence of MILO problems.

3. To the best of our knowledge, we are the first—in the field of vehicle repositioning research—to account for time-varying uncertainties in demand, travel destination, travel time, and repositioning duration. Our RnO model allows for realistic settings and is practically relevant.

4. We conduct extensive simulation experiments to demonstrate our model's efficacy. These experiments enable several observations. (i) Compared to benchmark models, our model achieves the highest average service level for a given repositioning cost budget. (ii) It is also robust to adversity in this sense: the worst-case service level is also the highest among tested models. (iii) vehicle-sharing networks benefit from the economies of scale.

The rest of this paper is organized as follows. After reviewing related research in Section 2, we describe the vehicle repositioning problem and offer a mathematical formulation of the dynamics and operational constraints in Section 3. In Section 4 we propose the robustness optimization model and show that we can obtain optimal solutions by solving a sequence of MILO problems. Our experimental studies are described in Section 5, after which we provide a brief summary and suggestions for future research in Section 6.

2. Literature review

Vehicle sharing is an emergent field in operations research and operations management; see Freund et al. (2019) for a comprehensive review of the literature on bike sharing, He et al. (2019) for a detailed summary of car sharing, and Hu (2018) for related literature and reviews on other aspects of sharing economy. Unlike most of these works (see also Nair and Miller-Hooks 2011, Liu et al. 2016, Ghosh et al. 2017, Schuijbroek et al. 2017, Li et al. 2018, Shui and Szeto 2018), our paper reviews the literature on vehicle repositioning problems primarily in terms of four aspects: modeling approach, model uncertainty, decision criteria, and spatial and temporal dependencies.

Modeling approach. Most of the vehicle-sharing literature employs deterministic or stochastic models. Among the papers with deterministic models, the majority formulate a MILO problem while focusing on the development of algorithms and heuristics (see e.g. Ho and Szeto 2014, Boyacı et al. 2015, O'Mahony and Shmoys 2015, Li et al. 2016, Liu et al. 2016, Ghosh et al. 2017, Freund et al. 2018, Shui and Szeto 2018). Another strand of literature models vehicle-sharing systems as closed queueing networks and uses steady-state approximations to evaluate system performance (George and Xia 2011, Fricker and Gast 2016, Banerjee et al. 2016, Braverman et al. 2019). To incorporate both the uncertainties and dynamics associated with a vehicle-sharing problem, scholars have developed models based on stochastic integer programming (Nair and Miller-Hooks 2011, Lu et al. 2017), network flow (Shu et al. 2013, Chou et al. 2019), Markov chain (Schuijbroek et al. 2017), dynamic programming (Benjaafar et al. 2017), robust optimization (Erera et al. 2009, Jian et al. 2016, He et al. 2018), survey analysis (Herrmann et al. 2014), and reinforcement learning (Li et al. 2018).

Our paper is related to Nair and Miller-Hooks (2011), where the authors use chance constraints to impose a fixed level of protection against violating operational constraints. Yet we use a riskiness index, rather than chance constraints, to minimize the risk of violating operational constraints. This approach yields bounds on the probability and magnitude of the constraint violation and, more importantly, is tractable. The RnO model can incorporate multi-dimensional uncertainties, whereas Nair and Miller-Hooks (2011) consider only the uncertainty of demand. Our RnO model can also be viewed as a "satisficing" model (Simon 1959, Brown and Sim 2009).

Model uncertainty. Demand is usually presumed to be uncertain. Most papers assume that demand follows a Poisson process (George and Xia 2011, Shu and Song 2013, Banerjee et al. 2016, Jian et al. 2016, Schuijbroek et al. 2017, Braverman et al. 2019, Chou et al. 2019); a few suppose that demand follows a general distribution (see e.g. Benjaafar et al. 2017, Lu et al. 2017, He et al. 2018). The travel time between any two locations is widely assumed to be exponentially distributed (Banerjee et al. 2016, Fricker and Gast 2016, Braverman et al. 2019), although some studies (e.g. George and Xia 2011) assume a general distribution. Both Braverman et al. and Benjaafar et al. suppose that a customer who arrives at one location will travel to another location with some certain probability. We believe that only Braverman et al.'s model incorporates uncertainty in the duration of repositioning.

Braverman et al. (2019) focus on car-sharing systems (e.g., Uber) and assume that repositioning time follows the same distribution as travel time. However, they can derive a steady-state policy only by assuming demand for rides (which is assumed to be a Poisson process) and supply of cars to be infinity—which is not realistic—so as to approximate the model via fluid-based optimization. Our robustness optimization model is flexible enough to incorporate different (and time-dependent) distributions for all relevant uncertainties. Our experimental study show that, for any given average repositioning cost, the robustness optimization model deliveries a higher service level than does a fluid-based optimization model.

Decision criteria. The decision criterion adopted for repositioning problems in vehicle-sharing systems is usually one of: minimizing cost (Nair and Miller-Hooks 2011, Ho and Szeto 2014, Nourinejad et al. 2015, Li et al. 2016, Benjaafar et al. 2017, Schuijbroek et al. 2017, He et al. 2018), maximizing profit (George and Xia 2011, Febbraro et al. 2012, Boyacı et al. 2015, Lu et al. 2017), minimizing unmet demand (Jian et al. 2016, Shui and Szeto 2018), maximizing the throughput (Shu et al. 2013, O'Mahony and Shmoys 2015, Banerjee et al. 2016, Chou et al. 2019), minimizing the user dissatisfaction function (Freund et al. 2019), or maximizing social welfare (Boyacı et al. 2015, Banerjee et al. 2016). In contrast, we model the problem from the perspective of robustness. Thus the RnO model, which can subsume most of the criteria just listed, aims to satisfy a variety of operational constraints to the greatest extent possible.

Spatial and temporal dependencies. In the presence of spatial and temporal dependencies, the likelihood of a trip's being completed depends both on its origin and on the volume of trips, which also depends on time and location (Benjaafar et al. 2017). Many papers consider time-dependent and location-dependent demand (see e.g., Febbraro et al. 2012, Shu et al. 2013, Ghosh et al. 2016, Benjaafar et al. 2017, He et al. 2018, Li et al. 2018, Shui and Szeto 2018). The RnO model considers not only such dependencies in demand but also travel time and the duration of repositioning.

Table 1 A summary of literature

Paper	Type of models	Uncertainties					Time Dependence
		Demand	Destination	Travel time	Reposition	Duration	
Banerjee et al. (2016)	4	√		√			
Benjaafar et al. (2017)	2	√	√	√			√
Boyacı et al. (2015)	1						
Braverman et al. (2019)	2	√	√	√	√		
Chou et al. (2019)	2	√					√
Chung et al. (2018)	4						
Erera et al. (2009)	3	√					
Febbraro et al. (2012)	4						√
Freund et al. (2019)	1						
Fricker and Gast (2016)	2	√		√			
George and Xia (2011)	2	√		√			
Ghosh et al. (2016)	3	√					
Ghosh et al. (2017)	1						√
He et al. (2018)	3	√					√
Herrmann et al. (2014)	4						
Ho and Szeto (2014)	1						
Jian et al. (2016)	2,4	√		√			
Kek et al. (2009)	4						
Li et al. (2016)	1						
Li et al. (2018)	4						√
Liu et al. (2016)	1						
Lu et al. (2017)	2	√					
Nair and Miller-Hooks (2011)	2	√					
Nourinejad et al. (2015)	1						
O'Mahony and Shmoys (2015)	1						
Schuijbroek et al. (2017)	2	√					
Shu et al. (2013)	2	√					√
Shui and Szeto (2018)	1						√
Our Paper	2,3	√	√	√	√		√

Model type: 1 for deterministic model, 2 for stochastic model, 3 for robust model, and 4 for others (simulation, predictive model, etc).

Table 1 summarizes the related literature in repositioning problems in vehicle-sharing systems, and it categorizes them based on the type of models, uncertainties, and time dependency. Unlike nearly all of the cited papers, which consider either a cost criterion (cost minimization, profit maximization) or partial uncertainties (demand, travel time), our paper is the first that we know of to integrate multi-dimensional and time-varying uncertainties into a model that addresses operational constraints from a robustness optimization perspective.

The repositioning problem is closely related to such classical transportation problems as rail-car distribution (Jordan and Turnquist 1983), empty container deployment (Crainic et al. 1993, Shu and Song 2013) and car rental logistics (Pachon et al. 2003) as well as the trans-shipment of inventories in supply chains (see e.g. Tagaras 1989, Robinson 1990, Rong et al. 2010). The model that we deploy here is also applicable to these problems.

3. Problem description and formulation

We consider a vehicle-sharing network in which an operator owns a fixed number M of vehicles and serves a well-defined region consisting of N locations over a planning horizon of T discrete periods. In each period, a random number of customers arrive at each location. They rent/pick up vehicles from one location and can return the vehicle at any location; thus both one-way and round trips are allowed. In this process, the operator faces two major sources of uncertainty: random demands and stochastic travel times. More specifically, the operator knows neither future demands nor the exact travel time of each ride, where the latter depends on the origin–destination pair and other covariate information such as traffic conditions. The operator can rely on historical data to infer the distributional information of demands and travel times, which may be inaccurate. Vehicles are *dispatched* to meet the demand based on a first-come, first-served policy. When there are no available vehicles at a location, the operator is unable to accommodate any further demands at this location in this period; the result is a loss of demand. In other words, we assume that customers are impatient so that demand does not accumulate over time.

So that demand can be better satisfied, the operator periodically reviews the remaining stock of vehicles at each location and determines how many vehicles to *reposition* among different locations. This repositioning decision plays a key role in improving the *service level*, which we define as the probability that customers will find available vehicles at their origins when they intend to travel (He et al. 2019). In sum, the decision maker must consider how current decisions may affect the system over the entire planning horizon—especially since the repositioning duration is uncertain. Before writing down the full model formally, we introduce system dynamics and operational constraints.

System dynamics

At the current period ($t = 1$), the planner observes the system's initial state—customer demand and the number of available vehicles at each location—before making *here-and-now* decisions on how to reposition vehicles in the network. Future uncertainties such as demands and travel times of individual trips only unfold gradually in future periods ($t = 2, \ldots, T$), and the planner can make some *recourse* repositioning decisions to adjust to the realizations of uncertainties. Figure 2 provides an illustration of how the system evolves over the planning horizon.

Operationally, this problem is solved in a rolling horizon fashion. In other words, only here-and-now decisions are implemented at the current period, and recourse decisions are modelling tools to evaluate or approximate future system dynamics. In order to obtain optimal here-and-now decisions, the planner must also find the optimal recourse policy. However, this is challenging because the optimal recourse policy can be any function of the realization of uncertainties. In this

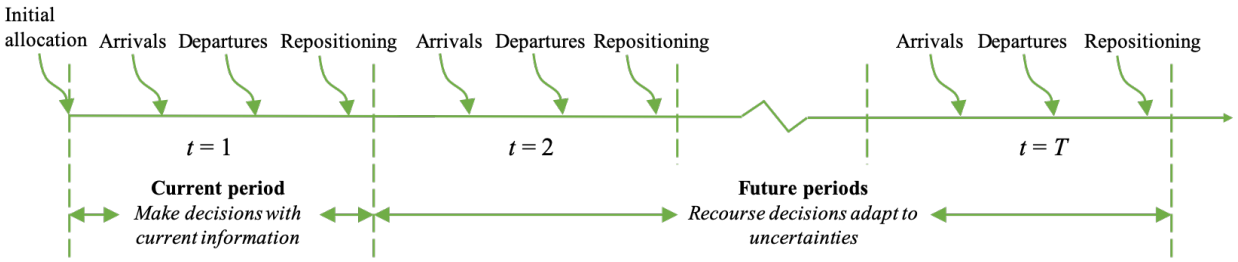

Figure 2 System Dynamics

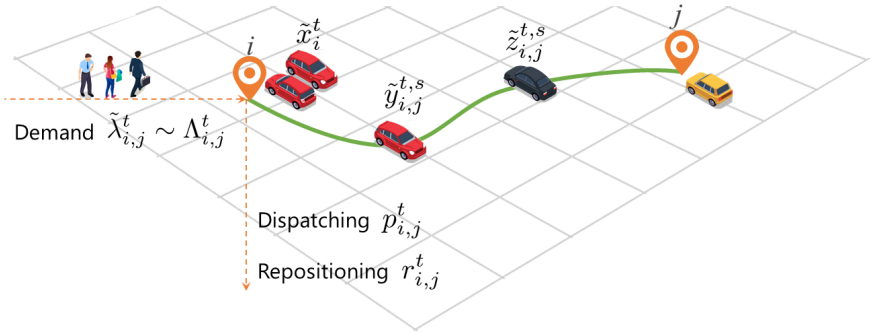

Figure 3 An illustration of the system at period t

paper, we restrict us to search only within the class of static recourse policies. This assumption will be made clearer as we gradually introduce the system dynamics below. We summarize notations in Table 2 and provide a schematic overview of the system at any period t in Figure 3.

We use $[a;b]$ to denote the set of running indices from a to $b>a$ (i.e., $\{a,a+1,\ldots,b\}$), and we let $[b] \triangleq [1;b]$ to ease the exposition. For any $t \in [T]$, the sequence of events is as follows. At the beginning of this period, vehicles that have completed their trips (from both repositioning and rental) arrive at each location. Then demand for transport from location $i \in [N]$ to location $j \in [N]$ is realized. At the current period ($t=1$), we use $\lambda_{i,j}^1$ to represent the observed demand. For future periods, we use $\tilde{\lambda}_{i,j}^t$ $(i,j \in [N], t \in [2;T])$ to denote the uncertain demand, and we assume that demand $\tilde{\lambda}_{i,j}^t$ is independent of other demands and its moment-generating function can be evaluated (cf. Lu et al. 2017, Banerjee et al. 2016). Hereinafter, we always use the tilde sign ($\tilde{}$) to denote random variables.

Let x_i^1 denote the number of vehicles at location i at the current period ($t=1$). Because our model is carried out in a rolling-horizon fashion, $\boldsymbol{x}^1$ can have two interpretations (we use boldface symbols to represent vectors). First, when the current period correspond to the start of daily operations, $\boldsymbol{x}^1$ represents the initial vehicle allocation and can be modeled as a decision variable under our framework. For ease of exposition, we assume in our main model that the initial allocation is already decided beforehand and is a given constant. Second, when the current period corresponds to a time

Table 2 Notation

Symbol	Description
	Parameters
M	Total number of vehicles in the system
N	Number of locations
T	Number of periods
S	Maximum travel time along any edge
$\mathcal{A}$	Adjacency set, i.e., $(i,j) \in \mathcal{A}$ if there is an edge (i,j) between locations i and j.
η	Service level
Γ	Cost budget
$\lambda_{i,j}^t$	Realized demand at location i at time t that is going to location j
$h_{i,j}^{t,s}$	Probability that a vehicle will arrive at j at period t *conditional* on it having traveled along edge (i,j) for $s-1$ periods at period $t-1$
$c_{i,j}^t$	Unit repositioning cost along edge (i,j) at time t
Δ_i^t	Capacity of location i at period t
	State and decision variables
x_i^t	Number of vehicles at location i at period t.
$p_{i,j}^t$	Number of vehicles needed to satisfy demand $\lambda_{i,j}^t$
$r_{i,j}^t$	Number of vehicles sent out for repositioning to j from i at time t
$y_{i,j}^{t,s}$	Number of vehicles that have been on the way, satisfying a demand from location i to location j, for s periods (which have not arrived yet) at period t
$z_{i,j}^{t,s}$	Number of vehicles that have been on the way for repositioning from location i to location j for s periods (which have not arrived yet) at period t

stamp within the daily operations, $\boldsymbol{x}^1$ represents the observed numbers of vehicles at all locations at the current period, which is known. Therefore, $\boldsymbol{x}^1$ is always treated as a constant parameter in our model. When $t \in [2;T]$, we use $\tilde{x}_i^t$ $(i \in [N])$ to denote the number of vehicles in location i at time t, which is a random variable that depends on repositioning decisions and the state of the system. This number $\tilde{x}_i^t$ includes all vehicles that arrived at the location i at time $1,\ldots,t$ and are *not* repositioned or dispatched before time t. We similarly use $p_{i,j}^t$ to denote the number of vehicles dispatched to fulfill the demand at time t—what we call the *dispatching decision*. We also let $r_{i,j}^t$ signify the number of vehicles that are sent for repositioning from location i to location j at time t.

We model the traffic along each edge (i,j), $(i,j) \in \mathcal{A}$, as a server whose service time is the same as the travel/transportation time. Observe that the travel time and the repositioning duration along the same edge (i,j) are likely to be different; therefore, we distinguish those times by treating them as two different servers. It is worth noting that in-traffic vehicles can be divided into different cohorts based on how long they have been in the "traffic arc". Following the notation of Bandi and Loke (2018), we let tracking time $s \in [0;S]$ characterize how long a vehicle has been in its current traffic arc; here S is the maximum possible travel time. We consider two sets of variables $y_{i,j}^{t,s}$ and $z_{i,j}^{t,s}$, which represent the number of vehicles at time t that have spent s periods along edge (i,j) in (respectively) a vehicle rental trip and repositioning process. By definition, $s=0$ indicates

that vehicles are just dispatched to edge (i,j). Hence $y_{i,j}^{t,0}$ and $z_{i,j}^{t,0}$ are the same as dispatching and repositioning decisions, respectively. Formally, we have

$$y_{i,j}^{t,0} = p_{i,j}^t \qquad \forall (i,j) \in \mathcal{A}, t \in [T], \tag{1}$$

$$z_{i,j}^{t,0} = r_{i,j}^t \qquad \forall (i,j) \in \mathcal{A}, t \in [T]. \tag{2}$$

In what follows, we will use $y_{i,j}^{t,0}, z_{i,j}^{t,0}$ directly instead of using $p_{i,j}^t, r_{i,j}^t$. For convenience, we let $\boldsymbol{y}^0, \boldsymbol{z}^0$ denote the vectors $(y_{i,j}^{t,0})_{(i,j)\in\mathcal{A},t\in[T]}$ and $(z_{i,j}^{t,0})_{(i,j)\in\mathcal{A},t\in[T]}$, respectively. When $t=1$ and $s \in [S]$, the number of vehicles in traffic is observed and known to the planner; that is, both $y_{i,j}^{1,s}$ and $z_{i,j}^{1,s}$ for all $s \in [S]$ are known constants. When $t \in [2;T]$ and $s \in [S]$, the number of vehicles in traffic is *not* observed by the planner. We use notation $\tilde{y}_{i,j}^{t,s}$ for all $t \in [2;T]$ and $s \in [S]$ to make it clear that these are random variables.

The term $h_{i,j}^{t,s}$ is used to denote the probability that a vehicle will arrive at location j at period $t+1$—provided it was dispatched to satisfy a demand along edge (i,j) in period $t-s$ and is still traveling at time t. Similarly, $d_{i,j}^{t,s}$ denotes the probability that a vehicle will arrive at j in period $t+1$ conditional on it being sent for repositioning along edge (i,j) at period $t-s$ and on it still traveling at time t. Both $h_{i,j}^{t,s}$ and $d_{i,j}^{t,s}$ are treated as hazard rates that can be directly estimated from historical data via survival analysis, which allows us to model arbitrary discrete service time distributions (Dai and Shi 2017).

ASSUMPTION 1. *Both travel time and repositioning duration along each edge $(i,j) \in \mathcal{A}$ are independent and identically distributed for different vehicles.*

Assumption 1 is realistic because different trips along the same edge are likely to be independent and follow the same travel time distribution (Banerjee et al. 2016). By Assumption 1, we can characterize how the number of vehicles in transit evolves in period t. First, each of the observed vehicles $y_{i,j}^{1,s}$ will independently complete the trip at time $t=2$ with probability $h_{i,j}^{1,s}$. We can resort to a binomial distribution to characterize $\tilde{y}_{i,j}^{2,s}$, writing $\tilde{y}_{i,j}^{2,s} \sim \text{Bin}(y_{i,j}^{1,s-1}, 1-h_{i,j}^{1,s-1})$ for all $(i,j) \in \mathcal{A}$ and $s \in [S]$. Analogously, $\tilde{z}_{i,j}^{2,s} \sim \text{Bin}(z_{i,j}^{1,s-1}, 1-d_{i,j}^{1,s-1})$ for all $(i,j) \in \mathcal{A}$ and $s \in [S]$. In general, the rest of the dynamics in traffic edges can be described in a similar way:

$$\tilde{y}_{i,j}^{t,s} \sim \text{Bin}(\tilde{y}_{i,j}^{t-1,s-1}, 1-h_{i,j}^{t-1,s-1}) \qquad \forall (i,j) \in \mathcal{A}, s \in [S], t \in [3;T];$$

$$\tilde{z}_{i,j}^{t,s} \sim \text{Bin}(\tilde{z}_{i,j}^{t-1,s-1}, 1-d_{i,j}^{t-1,s-1}) \qquad \forall (i,j) \in \mathcal{A}, s \in [S], t \in [3;T].$$

Again, this follows because each of the $\tilde{y}_{i,j}^{t-1,s-1}$ vehicles will, independently, complete the trip with probability $h_{i,j}^{t-1,s-1}$, or stay on the arc with probability $1-h_{i,j}^{t-1,s-1}$. In addition, the number of vehicles that successfully complete the trip from i to j at time $t \in [2;T]$ can be written as

$$\sum_{s\in[0;S]} \text{Bin}(\tilde{y}_{i,j}^{t-1,s}, h_{i,j}^{t-1,s}),$$

and the number of vehicles that are successfully repositioned along edge (i,j) is

$$\sum_{s\in[0;S]} \mathrm{Bin}(\tilde{z}_{i,j}^{t-1,s}, d_{i,j}^{t-1,s}).$$

We can now characterize the state transition of $\tilde{x}_{i,j}^t$ for $t\in[2;T]$:

$$\begin{aligned}\tilde{x}_i^t &= \tilde{x}_i^{t-1} - \sum_{j:(i,j)\in\mathcal{A}} y_{i,j}^{t-1,0} - \sum_{j:(i,j)\in\mathcal{A}} z_{i,j}^{t-1,0} + \sum_{j:(j,i)\in\mathcal{A}} \sum_{s\in[0;S]} (\mathrm{Bin}(y_{j,i}^{t-1,s}, h_{j,i}^{t-1,s}) + \mathrm{Bin}(z_{j,i}^{t-1,s}, d_{j,i}^{t-1,s})) \\ &= x_i^1 - \sum_{\tau\in[t-1]} \left(\sum_{j:(j,i)\in\mathcal{A}} y_{i,j}^{t-\tau,0} - \sum_{j:(i,j)\in\mathcal{A}} z_{i,j}^{t-\tau,0} \right) \\ &\quad + \sum_{\tau\in[t-1]} \sum_{j:(j,i)\in\mathcal{A}} \sum_{s\in[0;S]} (\mathrm{Bin}(y_{j,i}^{t-\tau,s}, h_{j,i}^{t-\tau,s}) + \mathrm{Bin}(z_{j,i}^{t-\tau,s}, d_{j,i}^{t-\tau,s})) \quad \forall t\in[2;T].\end{aligned}$$

The second equality results from the recursion over t. From this formulation, we can see that there is a random inflow of vehicles during each period and that the outflow consists only of decision variables. At the current period ($t=1$), there is no uncertainty, so the decision $y_{i,j}^{1,0}$ and $z_{i,j}^{1,0}$ are exact and directly implementable. However, for a future period t ($t\in[2;T]$), decisions $y_{i,j}^{t,0}$ and $z_{i,j}^{t,0}$, $(i,j)\in\mathcal{A}$, may depend on all realizations of primary uncertainties until time t.

Assumption 2. *We consider only static recourse variables, i.e., $y_{i,j}^{t,0}$ and $z_{i,j}^{t,0}$, for all $t\in[2;T]$ and $(i,j)\in\mathcal{A}$, are static variable.*

In general, it is difficult to characterize the true optimal recourse variables in a multi-stage optimization problem because they can be arbitrary functions of realized uncertain parameters. For tractability, we restrict ourselves to the static recourse variables to approximate the future dynamics. As we will show in the experimental study, this approximation can yield efficient and effective solutions. We remarks here that the recourse variables are not directly implementable, because its optimality and feasibility cannot be guaranteed for all future realizations. This issue is resolved when we implement the solutions in a rolling-horizon fashion.

Operational Constraints

Having defined the system dynamics, we can now model a variety of operational constraints and criteria that the operator must satisfy.

Service level. To maintain an overall service level η, the operator needs the following constraint to hold with high probability:

$$\sum_{(i,j)\in\mathcal{A}} \sum_{t\in[T]} y_{i,j}^{t,0} \geq \eta \sum_{(i,j)\in\mathcal{A}} \sum_{t\in[T]} \tilde{\lambda}_{i,j}^t. \tag{3}$$

Note that the service level can depend also on time (if we define η_t), location ($\eta_{i,j}$), or both ($\eta_{i,j}^t$). For example, the operator may require that the following time-dependent service level constraints—in addition to (3)—hold with high probability:

$$\sum_{(i,j)\in\mathcal{A}} y_{i,j}^{t,0} \geq \eta_t \sum_{(i,j)\in\mathcal{A}} \tilde{\lambda}_{i,j}^t \quad \forall t \in [T].$$

Capacity. For any location $i \in [N]$ and time $t \in [T]$, the total number of vehicles cannot exceed some capacity Δ_i^t. Therefore, the operator also seeks to route the network's vehicles such that the following capacity constraint holds with high probability:

$$\tilde{x}_i^t \leq \Delta_i^t \quad \forall i \in [N],\, t \in [T]. \tag{4}$$

Auxiliary constraints. Because we are using static recourse policies in future periods—that is, dispatching $y_{i,j}^{t,0}$ and repositioning $z_{i,j}^{t,0}$ for $(i,j) \in \mathcal{A}$, and $t \in [2:T]$—we must ensure these policies are feasible. First, the number of dispatched vehicles should not exceed demand for vehicles. Hence the following constraints should hold with high probability:

$$y_{i,j}^{t,0} \leq \tilde{\lambda}_{i,j}^t \quad \forall (i,j) \in \mathcal{A}, t \in [T]. \tag{5}$$

Then, the total number of vehicles used to satisfy demands and for repositioning from location i should not exceed the available vehicles at that location. Hence the following constraints should also hold with high probability:

$$\sum_{j:(i,j)\in\mathcal{A}} \left(y_{i,j}^{t,0} + z_{i,j}^{t,0}\right) \leq \tilde{x}_i^t \quad \forall i \in [N], t \in [T]. \tag{6}$$

Cost budget for repositioning. The operator may need to work within a cost budget Γ for repositioning. This cost budget constraint is a deterministic one and can be written as:

$$\sum_{(i,j)\in\mathcal{A}} \sum_{t\in[T]} c_{i,j}^t z_{i,j}^{t,0} \leq \Gamma, \tag{7}$$

where $c_{i,j}^t$ is unit cost for repositioning a vehicle along edge (i,j) at time t.

Additional deterministic linear constraints. It is straightforward for our model to incorporate many other practical operational constraints. For instance, an operator that views also the initial allocation as a decision can impose the constraints

$$\sum_{i\in[N]} x_i^1 \leq M \quad \forall (i,j) \in \mathcal{A},$$

where M is the total number of vehicles in the system.

These are deterministic linear constraints, so such constraints can be easily incorporated into our model without compromising tractability. In what follows, we do not explicitly write out these additional deterministic linear constraints. Instead, we let $(\boldsymbol{y}^0, \boldsymbol{z}^0) \in \mathcal{R}$ for a constrained set $\mathcal{R}$, which means they must satisfy a set of deterministic linear constraints. Notice that deterministic linear constraints do not contain random variables; therefore, they are "hard" constraints that must be satisfied under all circumstances.

Note that service level, capacity, and auxiliary constraints all involve random variables. Hence we must find some reasonable way to evaluate them and to ensure that they hold with high probability. One way is to recast these constraints as chance constraints (cf. Nair and Miller-Hooks 2011). Thus, for instance, we could impose the following chance constraint on capacity:

$$\mathbb{P}\left[\tilde{x}_i^t > \Delta_i^t\right] \leq \epsilon, \quad \forall i \in [N], t \in [T], \tag{8}$$

where ϵ is a probability bound in $(0, 1)$. However, chance constraints are not convex and so it is hard to derive a tractable reformation in general. We will therefore use a convex measure to evaluate the risk of constraint violation and approach these operational constraints from a robustness optimization perspective.

4. A robustness optimization model

Most of the literature balances potential lost sales and repositioning costs to minimize the total cost (see e.g. Benjaafar et al. 2017, He et al. 2018). Yet it can be impractical to quantify the total operational cost accurately, as we have mentioned in the introduction. To tackle the issue of inaccuracy in estimating the underlying probability distribution, some studies adopt the distributionally robust approach and evaluate the uncertainty as its worst-case expectation over an ambiguity set of possible probability distributions (see, e.g., He et al. 2018)—an approach that will likely produce conservative results. Under that approach, model performance depends also on the particular ambiguity set chosen and therefore provides no guarantee of performance *outside* the ambiguity set.

Motivated by Long et al. (2019), we propose a robustness optimization model for the vehicle repositioning problem, which seeks to satisfy (as much as possible) operational constraints (e.g., service level) while maintaining the operational cost within a specified budget. In practice, operational constraints are straightforward to define and some of our problem's chief constraints are identified in Section 3. Therefore, the RnO model is practical even when the operator finds it difficult to articulate monetary trade-offs among multiple criteria.

To characterize the risk of violating operational constraints, we employ the "adversarial impact measure" proposed by Long et al. (2019). We adopt the convention that $\inf \emptyset = +\infty$, where $\emptyset$ is the empty set.

Definition 1 (Adversarial Impact Measure). For a random variable $\tilde{\xi}$ on a support set $\mathcal{Z}$, a reference distribution $\hat{\mathbb{P}}$, and a budget τ, we define the *adversarial impact measure* as:

$$\rho(\tilde{\xi}-\tau) = \inf\left\{\alpha \geq 0 \mid \mathbb{E}_{\mathbb{P}}[\tilde{\xi}-\tau] \leq \alpha\Delta(\mathbb{P},\hat{\mathbb{P}}) \quad \forall \mathbb{P} \in \mathcal{P}_0(\mathcal{Z})\right\}, \tag{9}$$

Here $\mathcal{P}_0(\mathcal{Z})$ denotes the set of all probability distributions on a support set $\mathcal{Z}$, and $\Delta(\mathbb{P},\hat{\mathbb{P}})$ is a nonnegative function on the domain of probability distributions such that $\Delta(\mathbb{P},\hat{\mathbb{P}}) = 0$ if $\mathbb{P} = \hat{\mathbb{P}}$.

The adversarial impact measure has an interpretable physical meaning: it restrict the extent to which the random variable $\tilde{\xi}$ can exceed the budget τ when its distribution differs from the reference distribution. For example, $\tilde{\xi}$ could represent the total number of vehicles while the budget τ represents the capacity. Observe that

$$\mathbb{E}_{\mathbb{P}}[\tilde{\xi}] - \tau \leq \rho(\tilde{\xi})\Delta(\mathbb{P},\hat{\mathbb{P}}) \quad \forall \mathbb{P} \in \mathcal{P}_0(\mathcal{Z}).$$

Take $\Delta(\mathbb{P},\hat{\mathbb{P}})$ as a *probability-distance function* that measure how far a distribution $\mathbb{P}$ is from the reference distribution $\hat{\mathbb{P}}$. The adversarial impact measure serves to control the level of infeasibility whenever the actual probability distribution—an unknown distribution in the set of all possible probability distributions $\mathcal{P}_0(\mathcal{Z})$—is likely to deviate from the reference distribution $\hat{\mathbb{P}}$. This measure gives us a performance guarantee on the expected constraint violation as a function of how much the true probability distribution deviates from the reference. For example, if the true distribution is indeed the reference distribution (i.e., if $\mathbb{P} = \hat{\mathbb{P}}$), then the expected violation must be zero. Hence minimizing the adversarial impact measure over all possible solutions helps us identify the most robust solution that deviates from the reference probability distribution (i.e., the model misspecification) while always maintaining feasibility under that distribution.

Each operational constraint that involves uncertainties (e.g., (3) – (6)) is evaluated using the adversarial impact measure. The ith constraint is assigned the weight θ_i, after which we minimize the largest weighted adversarial impact measure subject to repositioning cost budget and other deterministic constraints. Thus we obtain the following model,

$$\begin{aligned}
&\min\ \alpha \\
&\text{s.t. } \rho\left(\sum_{(i,j)\in\mathcal{A}}\sum_{t\in[T]} \tilde{\lambda}^t_{i,j}\eta - \sum_{(i,j)\in\mathcal{A}}\sum_{t\in[T]} y^{t,0}_{i,j}\right) \leq \alpha\theta_1 \\
&\quad \rho\left(\tilde{x}^t_i - \Delta^t_i\right) \leq \alpha\theta_2 && \forall i\in[N],\ t\in[T] \\
&\quad \rho\left(\textstyle\sum_{j:(i,j)\in\mathcal{A}}\left(y^{t,0}_{i,j} + z^{t,0}_{i,j}\right) - \tilde{x}^t_i\right) \leq \alpha\theta_3 && \forall i\in[N],\ t\in[T] \\
&\quad \rho\left(y^{t,0}_{i,j} - \tilde{\lambda}^t_{i,j}\right) \leq \alpha\theta_4 && \forall (i,j)\in\mathcal{A},\ t\in[T] \\
&\quad \sum_{(i,j)\in\mathcal{A}}\sum_{t\in[T]} c^t_{i,j} z^{t,0}_{i,j} \leq \Gamma \\
&\quad \alpha \geq 0, \quad (\boldsymbol{y}^0, \boldsymbol{z}^0) \in \mathcal{R}.
\end{aligned} \tag{10}$$

One can view $\theta_1, \ldots, \theta_4$ as trade-off parameters that can be used to trade off among different operational constraints.

However, the tractability of Model (10) depends on our choice of probability distance function. For computational efficiency, we consider a specific form of the adversarial impact measure in which $\Delta(\mathbb{P}, \hat{\mathbb{P}})$ is given by the Kullback-Leibler (KL) divergence:

$$\Delta(\mathbb{P}, \hat{\mathbb{P}}) \triangleq D_{KL}(\mathbb{P} \| \hat{\mathbb{P}}) \triangleq \begin{cases} \mathbb{E}_{\mathbb{P}}[\log(\frac{\mathrm{d}\mathbb{P}}{\mathrm{d}\hat{\mathbb{P}}})] & \text{if } \mathbb{P} \ll \hat{\mathbb{P}} \\ \infty & \text{otherwise.} \end{cases}$$

For convenience, let $\hat{\mathbb{P}}$ denote the *reference* joint-distribution (here, a distribution estimated from data) for all state variables and let $\mathcal{Z}$ denote the support set of all state variables. Then Model (10) now can be written more explicitly as:

$$\begin{aligned}
&\min\ \alpha \\
&\text{s.t.} \sup_{\mathbb{P}\in\mathcal{P}_0(\mathcal{Z})} \left\{ \mathbb{E}_{\mathbb{P}}\left[\sum_{(i,j)\in\mathcal{A}} \sum_{t\in[T]} \tilde{\lambda}_{i,j}^t \eta - \sum_{(i,j)\in\mathcal{A}} \sum_{t\in[T]} y_{i,j}^{t,0} \right] - \alpha\theta_1 D_{\mathrm{KL}}(\mathbb{P}\|\hat{\mathbb{P}}) \right\} \le 0, \\
&\quad \sup_{\mathbb{P}\in\mathcal{P}_0(\mathcal{Z})} \left\{ \mathbb{E}_{\mathbb{P}}[\tilde{x}_i^t - \Delta_i^t] - \alpha\theta_2 D_{\mathrm{KL}}(\mathbb{P}\|\hat{\mathbb{P}}) \right\} \le 0 && \forall i \in [N],\, t \in [T], \\
&\quad \sup_{\mathbb{P}\in\mathcal{P}_0(\mathcal{Z})} \left\{ \mathbb{E}_{\mathbb{P}}\left[\sum_{j:(i,j)\in\mathcal{A}} (y_{i,j}^{t,0} + z_{i,j}^{t,0}) - \tilde{x}_i^t \right] - \alpha\theta_3 D_{\mathrm{KL}}(\mathbb{P}\|\hat{\mathbb{P}}) \right\} \le 0 && \forall i \in [N],\, t \in [T], \\
&\quad \sup_{\mathbb{P}\in\mathcal{P}_0(\mathcal{Z})} \left\{ \mathbb{E}_{\mathbb{P}}[y_{i,j}^{t,0} - \tilde{\lambda}_{i,j}^t] - \alpha\theta_4 D_{\mathrm{KL}}(\mathbb{P}\|\hat{\mathbb{P}}) \right\} \le 0 && \forall (i,j) \in \mathcal{A},]\, t \in [T], \\
&\quad \sum_{(i,j)\in\mathcal{A}} \sum_{t\in[T]} c_{i,j}^t z_{i,j}^{t,0} \le \Gamma, \\
&\quad \alpha \ge 0, \quad (\boldsymbol{y}^0, \boldsymbol{z}^0) \in \mathcal{R}.
\end{aligned} \tag{11}$$

According to Follmer and Schied (2002), for a real-valued function $\tilde{\xi}$ with a support set $\mathcal{Z}$ and two probability measures $\mathbb{P}, \hat{\mathbb{P}} \in \mathcal{P}_0(\mathcal{Z})$, we have

$$\sup_{\mathbb{P}\in\mathcal{P}_0(\mathcal{Z})} \{\mathbb{E}_{\mathbb{P}}[\tilde{\xi}] - \alpha D_{KL}(\mathbb{P}\|\hat{\mathbb{P}})\} = \alpha \log(\mathbb{E}_{\hat{\mathbb{P}}}[\exp(\tilde{\xi}/\alpha)]),$$

for any $\alpha > 0$. Hence, the first four sets of constraints in Model (11) can be equivalently written as

$$\phi_{\alpha\theta_1}\left(\sum_{(i,j)\in\mathcal{A}} \sum_{t\in[T]} \tilde{\lambda}_{i,j}^t \eta - \sum_{(i,j)\in\mathcal{A}} \sum_{t\in[T]} y_{i,j}^{t,0} \right) \le 0, \tag{12}$$

$$\phi_{\alpha\theta_2}\left(\tilde{x}_i^t - \Delta_i^t \right) \le 0 \qquad \forall i \in [N], t \in [T], \tag{13}$$

$$\phi_{\alpha\theta_3}\left(\sum_{j:(i,j)\in\mathcal{A}} \left(y_{i,j}^{t,0} + z_{i,j}^{t,0}\right) - \tilde{x}_i^t \right) \le 0 \qquad \forall i \in [N], t \in [T], \tag{14}$$

$$\phi_{\alpha\theta_4}\left(y_{i,j}^{t,0} - \tilde{\lambda}_{i,j}^t \right) \le 0 \qquad \forall (i,j) \in \mathcal{A}, t \in [T], \tag{15}$$

where we define $\phi_\alpha(\tilde{\xi}) \triangleq \alpha \log\left(\mathbb{E}_{\hat{\mathbb{P}}}[\exp(\tilde{\xi}/\alpha)]\right)$. Similar measures are used in several recent paper, see, e.g., Jaillet et al. (2016), Adulyasak and Jaillet (2016).

For convenience, we shall call above constraints the *resilience* constraints. Constraint (12) and (13) are the resilience counterparts of (respectively) service level constraint (3) and capacity constraint (4). According to (14), the total number of vehicles to be dispatched and to be repositioned should not exceed the number of available vehicles at any location i. By constraint (15), we cannot create demands—in other words, we cannot have negative lost sales. By the definition of the adversarial impact measure, these constraints are robust to ambiguity in the underlying probability distribution; that is, the expected constraint violation is bounded when the actual distribution differs from the reference distribution $\hat{\mathbb{P}}$. Furthermore, the resilience constraints provide (theoretical) guarantees on both the probability and expected magnitude of constraint violation under the reference distribution $\hat{\mathbb{P}}$.

PROPOSITION 1 **(Guarantees under the reference distribution)**. *For any random variable $\tilde{\xi}$ such that $\rho(\tilde{\xi}) \in (0, +\infty)$, we have two bounds as follow.*

1. *Probability bound:* $\hat{\mathbb{P}}(\tilde{\xi} > \tau + \epsilon) \leq \exp(-\epsilon/\rho(\tilde{\xi}))$.
2. *Expectation bound:* $\mathbb{E}_{\hat{\mathbb{P}}}[(\tilde{\xi} - \tau - \epsilon)^+] \leq \frac{\rho(\xi)}{e} \exp(-\epsilon/\rho(\xi))$.

Proof. The first one follows from the Chernoff bound and is also presented in Hall et al. (2015). The second one follows because $\xi^+ \leq \exp(\xi - 1)$ and is also presented in Xie et al. (2017). □

Hence we arrive at the following *robustness optimization model*:

$$\begin{aligned} &\inf\ \alpha \\ &\text{s.t. Resilience constraints (12)} - \text{(15)}, \\ &\quad \sum_{(i,j)\in\mathcal{A}} \sum_{t\in[T]} c_{i,j}^t z_{i,j}^{t,0} \leq \Gamma, \\ &\quad \alpha > 0, \quad (\boldsymbol{y}^0, \boldsymbol{z}^0) \in \mathcal{R}. \end{aligned} \tag{16}$$

Note that $\lim_{\alpha\to+\infty} \phi_\alpha(\tilde{\xi}) = \mathbb{E}_{\hat{\mathbb{P}}}[\tilde{\xi}]$ for any $\tilde{\xi} \sim \hat{\mathbb{P}}$, and $\lim_{\alpha\to 0} \phi_\alpha(\tilde{\xi}) = \text{esssup}(\tilde{\xi})$. We can easily check whether the robustness optimization model is feasible for some $\alpha < +\infty$ by checking whether all operational constraints hold in expectation. In practice, the operator should set reasonable operational targets and constraints that are reasonable enough to be achieved in expectation. In that event, we can safely assume that the RnO model (16) is feasible.

Our objective is to minimize α, so Problem (16) can be solved via a bisection search on $\alpha > 0$. This search proceeds as follows.

1. Initialize α_h to be a large number and α_l to be a small number such that the resilience constraints are feasible under α_h but infeasible under α_l.

2. Set $\alpha = (\alpha_h + \alpha_l)/2$ and then solve the following subproblem:

$$\begin{aligned} &\inf\ 0 \\ &\text{s.t. Resilience constraints } (12)-(15) \text{ for above defined } \alpha, \\ &\sum_{(i,j)\in\mathcal{A}} \sum_{t\in[T]} c_{i,j}^t z_{i,j}^{t,0} \le \Gamma, \\ &(\boldsymbol{y}^0, \boldsymbol{z}^0) \in \mathcal{R}. \end{aligned} \tag{17}$$

3. If subproblem (17) is infeasible then set $\alpha_l = \alpha$ and keep α_h the same; otherwise, set $\alpha_h = \alpha$ and keep α_l the same.

4. Stop the procedure whenever $\alpha_h - \alpha_l \le \epsilon$ for $\epsilon > 0$ a preset (and positive) small number. Otherwise, return to step 2.

It follows that Problem (16) can be efficiently solved as long as subproblem (17) can be efficiently evaluated.

Tractable Reformulation

Here, we demonstrate that each constraint of Problem (17) is affine in either $\boldsymbol{y}^0$ or $\boldsymbol{z}^0$ (or both), and thus Problem (17) can be solved efficiently. We start by reformulating the resilience constraints for a given α.

PROPOSITION 2 **(Service level)**. *Constraint* (12) *can be reformulated as an affine constraint in* $\boldsymbol{y}^0$ *for any given* α*:*

$$\phi_\alpha\left(\sum_{(i,j)\in\mathcal{A}}\sum_{t\in[T]} \tilde{\lambda}_{i,j}^t \eta - \sum_{(i,j)\in\mathcal{A}}\sum_{t\in[T]} y_{i,j}^{t,0}\right) = \sum_{(i,j)\in\mathcal{A}}\sum_{t\in[T]} \phi_\alpha(\tilde{\lambda}_{i,j}^t \eta) - \sum_{(i,j)\in\mathcal{A}}\sum_{t\in[T]} y_{i,j}^{t,0}. \tag{18}$$

An edge-specific and/or time-specific service level constraint can be similarly reformulated. For example,

$$\phi_\alpha\left(\tilde{\lambda}_{i,j}^t \eta_{i,j}^t - y_{i,j}^{t,0}\right) = \phi_\alpha(\tilde{\lambda}_{i,j}^t \eta_{i,j}^t) - y_{i,j}^{t,0}, \quad (i,j)\in\mathcal{A}, t\in[T].$$

PROPOSITION 3 **(Capacity)**. *Constraints in* (13) *can be reformulated as affine constraints in* $\boldsymbol{y}^0$ *and* $\boldsymbol{z}^0$ *for any given* α*. More specifically,*

$$\begin{aligned} &\phi_\alpha\left(\tilde{x}_i^t - \Delta_i^t\right) \\ =&x_i^1 - \sum_{j:(i,j)\in\mathcal{A}}\sum_{\tau=1}^{t-1}(y_{i,j}^{\tau,0} + z_{i,j}^{\tau,0}) + \sum_{j:(j,i)\in\mathcal{A}}\sum_{\tau=1}^{t-1} y_{j,i}^{\tau,0}\delta_{j,i}^{\tau,t} + \sum_{j:(j,i)\in\mathcal{A}}\sum_{\tau=1}^{t-1} z_{j,i}^{\tau,0}\beta_{j,i}^{\tau,t} \\ &+ \sum_{j:(j,i)\in\mathcal{A}}\sum_{\tau=0}^{S-1} y_{j,i}^{1,\tau+1}\omega_{j,i}^{\tau,t} + \sum_{j:(j,i)\in\mathcal{A}}\sum_{\tau=0}^{S-1} z_{j,i}^{1,\tau+1}\kappa_{j,i}^{\tau,t} - \Delta_i^t \end{aligned}$$

where $\boldsymbol{\delta}$, $\boldsymbol{\beta}$, $\boldsymbol{\omega}$, *and* $\boldsymbol{\kappa}$ *are constant parameters defined in the Appendix. These parameters are independent of the decision variables.*

The proof of Proposition 3 is representative for the techniques we use; interested reader can refer to the Appendix A for details.

The final reformulation in Proposition 3 seems complicated, but it has advantage of being affine in the dispatching variables $\boldsymbol{y}^0$ and the repositioning variables $\boldsymbol{z}^0$. Therefore, the capacity constraints can be evaluated efficiently for any given α. The constants $\boldsymbol{\delta}$, $\boldsymbol{\beta}$, $\boldsymbol{\omega}$, and $\boldsymbol{\kappa}$ capture the degree of robustness through parameter α. A larger α is consistent with more risk neutrality. For example, $\lim_{\alpha\to+\infty} \delta^\tau_{i,j} = \sum_{s=0}^{\tau-1} \hat{h}^{\tau+s,s}$. In other words, this limit is the expected proportion of vehicles that will complete the trip under the reference distribution $\hat{\mathbb{P}}$. A larger α corresponds to less ambiguity aversion, as follows from the definition of the adversarial impact measure. Conversely, a smaller α corresponds to more ambiguity aversion; it also corresponds to greater risk aversion: $\lim_{\alpha\to 0} \delta^\tau_{i,j} = 1$.

PROPOSITION 4 **(Dispatching and repositioning)**. *The constraints in* (14) *can be reformulated as affine constraints in* $\boldsymbol{y}^0, \boldsymbol{z}^0$ *for any given* α*:*

$$\begin{aligned}
&\phi_\alpha\Bigg(\sum_{j:(i,j)\in\mathcal{A}} \left(y^{t,0}_{i,j} + z^{t,0}_{i,j}\right) - \tilde{x}^t_i\Bigg) \\
&\quad = \sum_{j:(i,j)\in\mathcal{A}} \sum_{\tau=1}^{t} (y^{\tau,0}_{i,j} + z^{\tau,0}_{i,j}) - x^1_i + \sum_{j:(j,i)\in\mathcal{A}} \sum_{\tau=1}^{t} y^{\tau,0}_{j,i} \bar{\delta}^{\tau,t+1}_{j,i} + \sum_{j:(j,i)\in\mathcal{A}} \sum_{\tau=1}^{t} z^{\tau,0}_{j,i} \bar{\beta}^{\tau,t+1}_{j,i} \\
&\qquad + \sum_{j:(j,i)\in\mathcal{A}} \sum_{\tau=0}^{S-1} y^{1,\tau+1}_{j,i} \bar{\omega}^{\tau,t+1}_{j,i} + \sum_{j:(j,i)\in\mathcal{A}} \sum_{\tau=0}^{S-1} z^{1,\tau+1}_{j,i} \bar{\kappa}^{\tau,t+1}_{j,i};
\end{aligned}$$

here $\bar{\boldsymbol{\delta}}$, $\bar{\boldsymbol{\beta}}$, $\bar{\boldsymbol{\omega}}$, *and* $\bar{\boldsymbol{\kappa}}$ *are constant parameters defined in the Appendix and are independent of decision variables.*

PROPOSITION 5 **(Dispatching)**. *The constraints in* (15) *can be reformulated as affine constraints in* $\boldsymbol{y}^0$ *for any given* α*. In particular,*

$$\phi_\alpha\left(y^{t,0}_{i,j} - \tilde{\lambda}^t_{i,j}\right) = y^{t,0}_{i,j} + \phi_\alpha(-\tilde{\lambda}^t_{i,j})$$

Proof. This equations holds trivially. The second term on the right hand side is a constant for any given α. □

We finally arrive at the following Theorem, which entails that Model (16) can be efficiently solved using available commercial solvers.

THEOREM 1. *Model* (16) *can be reformulated and solved via a bisection search in which each subproblem is a mixed-integer linear optimization problem.*

Proof. As discussed previously, Model (16) can be solved via a bisection search. Our reformulations imply that subproblem (17) is, in effect, a mixed-integer linear programming problem that can be solved efficiently. □

We remark that Bandi and Loke (2018) propose a framework for flow control in queuing networks in which also the node time s is tracked. There are several differences, in terms of modeling, between Bandi and Loke (2018) and our study.

1. The vehicle-sharing system is not readily a queueing network as described in Bandi and Loke (2018). We do not have typical queues at which jobs (demands) arrive; instead, we only have a buffer that stores all available "inventory" of vehicles. Bandi and Loke (2018) mainly study how to optimally route jobs in the system so as to improve their service experience. However, jobs in our model are immediately matched to vehicles and stochastically route some vehicles across the network. Because jobs are exogenous, the destinations of vehicles matched to the jobs are independent of decisions. We aim to optimally route (reposition) empty vehicles at the same time. In other words, our focus is not on how and when to handle demands but allocating the "inventory" of vehicles over time to better match supply and demand. For each traffic edge we create two different servers: one that processes user trips and another that processes repositioning trips. The process of repositioning vehicles is stochastic, state-dependent, and decision-dependent. It is not obviously ex ante how best to devise a tractable construction of this network, and we propose a high-fidelity approach.

2. The RnO model can be seen as a two-stage model and aims to derive here-and-now dispatch and repositioning decisions. The only reason to construct the traffic network in this way is so that we can easily approximate future dynamics. In addition, this model is carried out in a rolling horizon fashion in our numerical study, demonstrating its efficiency in a dynamic setting.

3. In the proof of proposition 3, we encounter a summation of dependent random variables and explicitly reformulate them into a tractable format. Furthermore, we simplify the notation by omitting the node time s from the state variable $\tilde{\boldsymbol{x}}$ in the reformulation.

5. Experimental study

We conduct simulation studies under various settings in order to elucidate the effectiveness of our model in improving operations and also to demonstrate the model's computational efficiency and robustness. Thus we focus on answering these four questions related to different practical aspects of vehicle-sharing problems.

1) What is the performance gap between our model and some benchmark models (e.g. the deterministic model) in terms of service level and repositioning cost?

2) Is our model computationally efficient?

3) What are the effects of network size and repositioning frequency?

4) How does our model perform as compared with the fluid-based optimization model presented by Braverman et al. (2019)?

In what follows, we describe the setting of our experimental study and then deliver insights into these practical questions. The studies were performed using a desktop computer with 64 GB of RAM and a 2.1-GHz CPU.

Parameter settings. In the basic setting, we consider a planning horizon of $T = 10$ periods on a complete graph with $N = 10$ nodes representing locations. We randomly and uniformly generate the locations of these 10 nodes on a 100×100 lattice grid. For each arc $(i, j) \in \mathcal{A}$, we let the demand at period $t \in [T]$ follow a Poisson distribution with mean value $\lambda_{i,j}^t = D \times i/N$, where the maximum mean demand $D = 20$. In this way we create unbalanced mean demands $2, 4, \ldots, 20$ for arcs departing from respective nodes $1, 2, \cdots, 10$, respectively. Now let the unit traveling cost of each arc $(i, j) \in \mathcal{A}$ be $c_{i,j}^t = 0.01 \times d_{i,j}$ for $d_{i,j}$ its Euclidean distance, and set the cost budget $\Gamma = 300$. Since empirical studies show that lognormal distributions fit well with travel times (Richardson and Taylor 1978, Srinivasan et al. 2014), we let the travel time at $t \in [T]$ follows a discrete and truncated lognormal distribution with mean $\log(\mu_{i,j}^t)$ and standard deviation $\mu_{i,j}^t/7$, where $\mu_{i,j}^t$ is generated by $\mu_{i,j}^t = 5 \times d_{i,j}/H$ and where $H = 100\sqrt{2}$ is the length of the plane's diagonal line. In this setting, the mean travel time is bounded from above at 5 periods. For each location $i \in [N]$, we set the number of initial available vehicles $X_i = D \times N \times 1.2 = 240$ and the capacity $\Delta_i^t = 1.2 \times X_i = 288$ for $t \in [T]$. We let the prescribed service level be $\eta_t = 0.98$ for $t \in [T]$. If model (16) is not feasible under this service level, then we reduce η_t in increments of 0.02 until the model *is* feasible. This is a reasonable procedure because, in practice, the operator will set a service level that is achievable.

To evaluate our model's performance, we conduct the experiments in a rolling horizon manner. So in each run, we consider a rolling window of 10 periods. That is: when we generate a sample path, it comprises realized demands and travel times over 10 periods—even though they are only revealed sequentially over time. Given the realization of the first-period demands, we solve the robustness optimization problem for the system's initial state: all vehicles are at rental locations, and none is on an arc. We fulfill the demands to the greatest extent and make the repositioning decisions for the remaining vehicles (if any). Though we obtain the dispatching and repositioning decisions for the entire 10 periods, we implement decisions only at the current period. The system then evolves into the next period, at which point we solve the problem again with the updated system state. This process is repeated until the 10th period, after which we evaluate the model performance for that run. We run 20 simulations with each simulation having one sample path and then report the average model performance.

In these experiments, we are concerned with the system service level in light of the total repositioning cost budget. This performance metric is both easy to evaluate and widely used in practice. For example, the operator of Citi Bike is under service-level agreements with the NYC Department

of Transportation (Banerjee et al. 2016). We compare the performance of our robustness optimization model with that of baseline models based on the same 20 sample paths. The baseline models are described as follows:

- *No reposition model.* No repositioning occurs at any period.
- *A priori model.* We solve the robustness optimization problem and obtain solutions for the entire 10 periods. From the second period onwards, instead of solving the problem again we simply plug in the previous derived solutions. Note that future-period solutions may not be integer; in that event, we round them to the nearest integer.
- *Deterministic model.* In this model, the operator presumes that unobserved future demands and travel times are the same as their expected values.
- *Partial-deterministic (Partial-D) model.* Recall that if α is large enough ($\alpha \to +\infty$) then $\phi_\alpha(\cdot)$ is essentially the same as the expectation. The partial-deterministic model solves Problem (17) while fixing a sufficiently large α. This model has a simple physical interpretation: demands are evaluated as their expected values although travel times remain uncertain. Yet when α is sufficiently large, the number of trip completions ending at any location during any period is evaluated as the expected number based on the travel time distribution. We therefore call this the partial-deterministic model.

All solutions of the latter two baseline models—like those of the robustness optimization model we propose—are solved and implemented in a rolling horizon fashion.

Efficient frontier. We first vary the total cost budget among the values $\{20, 50, 100, 200, 300, 400, 500\}$ to obtain average service level and average repositioning cost. In addition, we obtain the maximum number of unmet customer requests over all the sample paths for each cost budget and refer to this number as the *maximum violation*. We then evaluate the efficient frontiers of our focal models and plot them in Figure 4, where the horizontal axis represents the (normalized) average repositioning cost and the vertical axises correspond to the average service level (left panel) and maximum violation (right panel).

Among these models, the no reposition model outputs the lowest average service level and largest maximum violations, followed by the a priori model. The gap of these two models, however, is rather huge. On average, the improvement in service level of the a priori model (as compared to the no reposition model) is 25.5%, and the improvement in terms of maximum violation metric is 32%. These observations demonstrate the value of repositioning: large improvement in service level and huge reduction in maximum violation.

The other three models are all executed in a rolling horizon fashion and with the same repositioning cost budget. Figure 4 demonstrates that all the other three models have higher average

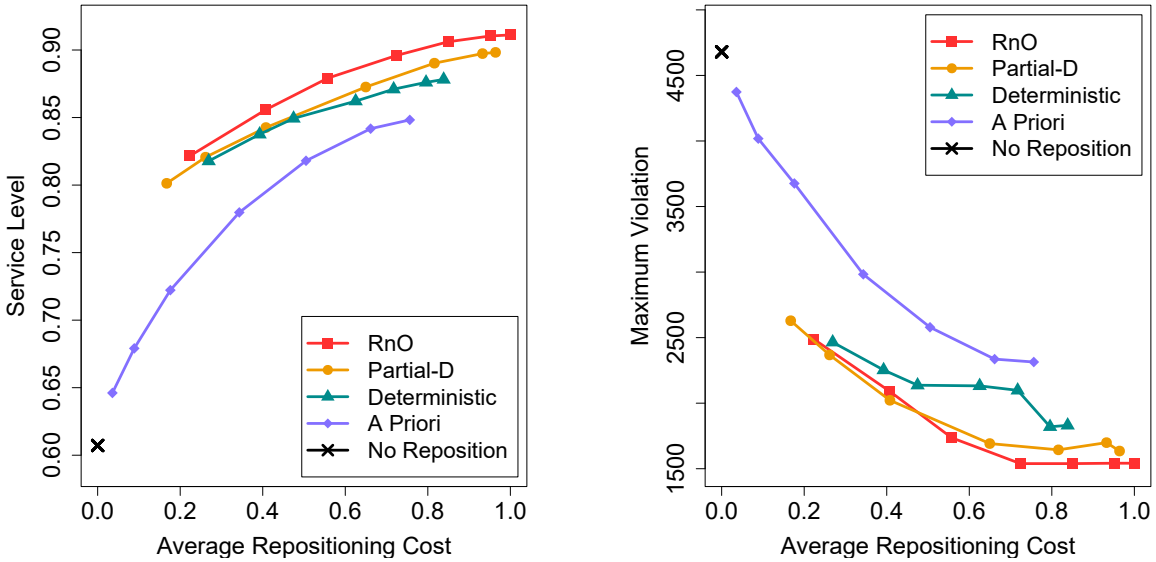

Figure 4 Efficient frontier: service level (left panel) and maximum violation (right panel) w.r.t. average repositioning cost

service level and lower maximum violation for a given average repositioning cost. This outcome is intuitive because the a priori model does not fully utilize available information. In other words, information updating is of great value in dynamic repositioning under uncertainty. Hence a model that is executed in a rolling horizon manner can reduce unmet demand and thereby significantly improve the service level.

The average service level of the partial-D model is higher than that of the deterministic model because the former accounts for travel time uncertainties and latter disregards any uncertainty in the system. The average service level of our RnO model is likewise higher than that of the partial-D model because we account for uncertainty also in demand. The improvement in average service level (as compared to the deterministic model) can be 3.1% on average.

Our RnO model achieves the lowest maximum violation, which means that it is the most robust to adverse circumstances. This robustness reflects the objective of our RnO model, which is designed to find the least risky solutions such that—to the greatest possible—service levels are achieved while observing operational constraints. Thus solution hedges strongly against adversity. The improvement in terms of our maximum violation metric—as compared to the deterministic model—can be 15.3% on average.

Computational efficiency. Table 3 reports the average computational time of the deterministic, a priori, partial-D, and RnO models in terms of the number of locations. Although the RnO

model's computational time increases quickly with the number of locations, the resulting time is still acceptable.

Table 3 Computational time of different models

Locations	Computational time (s)				
	Deterministic (MILP)	A priori (MILP)	Partial-D (MILP)	RnO (MILP)	RnO (LP)
5	0.02	0.28	0.03	0.24	0.18
10	0.10	1.23	0.16	1.17	0.85
20	0.55	6.92	1.05	7.14	4.14
30	1.41	23.03	3.49	24.65	10.44
40	3.70	60.37	9.85	69.04	20.71
50	7.86	136.04	22.00	171.87	38.60

We also consider the *linear programming (LP) relaxation model*, in which all the RnO model's decision variables are set to be continuous and then the first-period decisions are rounded to the nearest integers for implementation. As shown in Table 3, the LP relaxation model can be solved much more rapidly than can the RnO model. Perhaps more interesting is that, as shown in Table 4, the performance gap between these two models—in terms of both service level and repositioning cost—is almost negligible in our experimental instances. In practice, one can directly implement the LP relaxation model.

Table 4 Performance gap between the RnO model and that of its LP relaxation counterpart

Locations		5	10	20	30	40	50
Service Level	RnO	0.87	0.91	0.93	0.94	0.95	0.96
	LP	0.10%	-0.06%	-0.03%	-0.13%	-0.09%	-0.06%
Repositioning Cost	RnO	132.96	477.83	1782.86	4033.68	6816.32	10496.96
	LP	0.76%	0.74%	0.63%	-0.82%	-0.02%	0.66%

Impact of network size We now test how network size affects both the service level and the repositioning cost, where the *size* of a network is defined as its number of locations. Figure 5 plots the service level and the marginal repositioning cost—where the latter is defined as the average cost per arc—with respect to the network size. This graph shows that the larger the network, the higher the service level; in contrast, the marginal repositioning cost manifests a decreasing trend. A plausible explanation is that the total number of vehicles increases with network size. Thus we exploit the benefit of risk-pooling, and the operator is more likely to reposition vehicles among nearby locations. In other words, a vehicle-sharing network benefits from economies of scale.

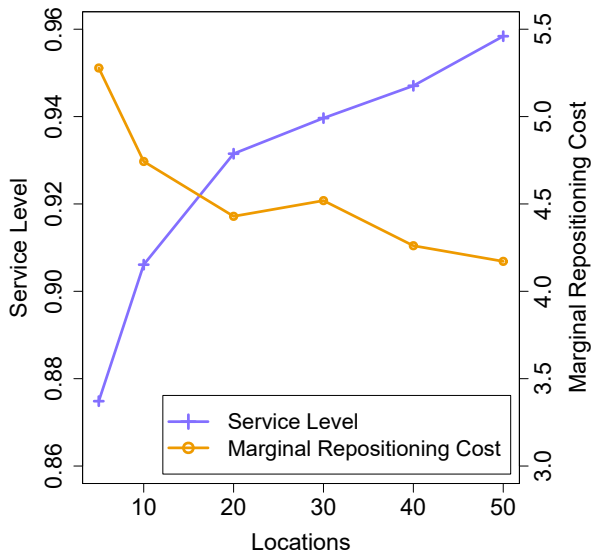

Figure 5 Service level and marginal repositioning cost w.r.t. number of locations

Impact of repositioning frequency. In practice, it might be costly to reposition in each period—especially when, as in a bike-sharing system, each period lasts only a few minutes. The operator will naturally want to know how service level changes with repositioning frequency for a given cost budget. We test different frequencies at which the vehicle-sharing system can reposition vehicles, where that repositioning interval is allowed to range from 1 to 5 periods; For example, if the repositioning interval is 2, we then only reposition at period 1, 3, 5, 7, and 9. We benchmark on the full model—repositioning interval is 1 period, and calculate the percentage of change in service level when the repositioning interval increases; the results are presented in Figure 6.

This finding is intuitive—the more frequent an operator repositions, the higher the service level can be. As the figure shows, repositioning vehicles every 5 periods results in a 9.1% loss in average service level when compared with repositioning vehicles each period. A lower target service level allows the owner to reposition vehicles less often.

Comparison with Braverman et al. (2019) Here we compare our RnO model with the most recent fluid-based optimization model (FbO) described by Braverman et al. (2019). These authors employ queueing theory to investigate the problem of repositioning empty cars. They consider a closed queueing network model, prove that it converges to a fluid limit when demand and supply tend to infinity, and use their FbO to establish an upper bound on the network model. In essence, this model yields a constant policy—the proportion of vehicles to be repositioned in each period at each location—that is non-adaptive to the system status. The fluid-based optimization model is presented formally in Appendix B; see Braverman et al. (2019) for additional details.

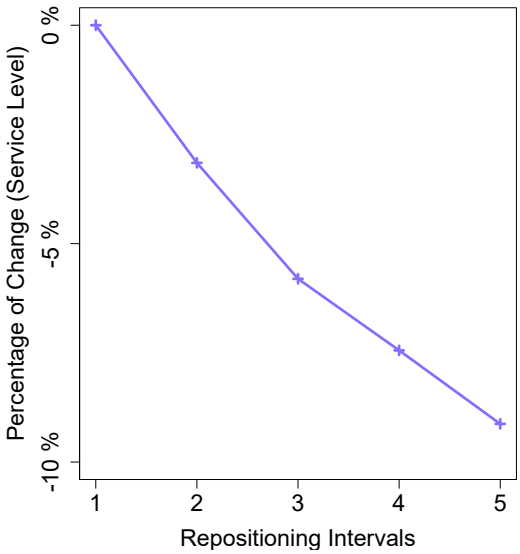

Figure 6 Percentage of change w.r.t. the repositioning intervals

Note that the FbO model does not include a cost budget. To enable a fair comparison, in each period, we obtain a solution from the FbO model and then implement it to obtain the average cost. We use this cost as our cost budget, so that both the RnO and FbO models have nearly the same average cost, and evaluate their respective service level under different network size. The results are given in Table 5.

Table 5 Comparison of FbO and RnO simulation results

Locations	Average Repositioning Cost			Service Level		
	FbO	RnO	RnO (%)	FbO	RnO	RnO (%)
5	134.27	128.23	-4.50	0.82	0.88	7.12
10	482.72	482.28	-0.09	0.85	0.91	6.17
20	1850.72	1850.69	0.00	0.89	0.93	5.07
30	4260.78	4260.76	0.00	0.90	0.94	4.44
40	6757.40	6757.38	0.00	0.91	0.95	4.67
50	9848.93	9848.90	0.00	0.92	0.96	3.97

This table reveals that, the RnO mode is most likely to utilize all the cost budget. For almost the same average cost and across all location configurations, our RnO model outputs a higher service level than does the RbO model; the improvement ranges between about 3.97 and 7.12 percent. It is worth emphasizing that the FbO model must assume a Poisson process for the arrival whereas our model is applicable to any demand distributions with finite moment generating functions. Finally, the FbO model amounts to a steady-state convergence of the queueing network whereas our model is time-dependent yet flexible enough to incorporate various operational constraints.

6. Concluding Remarks

We consider the general repositioning problem in vehicle-sharing systems. Addressing this problem involves a host of challenges that include time-dependent and multi-dimensional uncertainties in the system as well as multiple operational constraints that must be satisfied. We propose a high-fidelity model to tackle these real-world challenges. More specifically, we adopt Long et al.'s adversarial impact measure to characterize the risk of violating operational constraints. We then propose a robustness optimization model and show that its solution consists of solving a sequence of mixed-integer linear optimization problems.

We conduct an experimental study to demonstrate the computational efficacy and scalability of our RnO model. This study allows us to draw the following conclusions. (i) When compared with various benchmarks, such as deterministic model, our RnO model achieves the highest average service level for any given repositioning cost budget. (ii) The RnO model also is robust to adversity; that is, its worst-case service level is higher than that of all the benchmark models. (iii) Vehicle-sharing networks benefit from the economies of scale. (iv) Our robustness optimization model delivers a higher service level than does the fluid-based optimization model proposed by Braverman et al. (2019).

There are at least two important directions that have yet to be explored fully. First, how to design incentive programs and combine it with repositioning policies to balance the demand and supply effectively in vehicle-sharing systems? Second, how should pricing decisions in such systems be affected by consideration of the various uncertainties and operational constraints?

Acknowledgments

The authors are thankful to Melvyn Sim and Gar Goei Loke whose comments have resulted in a significant improvement to the original draft.

References

Adulyasak, Yossiri, Patrick Jaillet. 2016. Models and algorithms for stochastic and robust vehicle routing with deadlines. *Transportation Science* **50**(2) 608–626.

Bandi, Chaithanya, Gar Goei Loke. 2018. Exploiting hidden convexity in queueing networks: A novel approach to optimal control of flows. Available at: https://ssrn.com/abstract=3190874.

Banerjee, Siddhartha, Daniel Freund, Thodoris Lykouris. 2016. Pricing and optimization in shared vehicle systems: An approximation framework. Available at: arXivpreprintarXiv:1608.06819 .

Benjaafar, Saif, Xiang Li, Xiaobo Li. 2017. Inventory repositioning in on-demand product rental networks. Available at: https://ssrn.com/abstract=2942921 .

Boyacı, Burak, Konstantinos G Zografos, Nikolas Geroliminis. 2015. An optimization framework for the development of efficient one-way car-sharing systems. *European Journal of Operational Research* **240**(3) 718–733.

Braverman, Anton, Jim G Dai, Xin Liu, Lei Ying. 2019. Empty-car routing in ridesharing systems. *Operations Research* **67**(5) 1437–1452.

Brown, David B, Melvyn Sim. 2009. Satisficing measures for analysis of risky positions. *Management Science* **55**(1) 71–84.

Chou, Mabel C, Qizhang Liu, Chung-Piaw Teo, Deanna Yeo. 2019. Models for effective deployment and redistribution of shared bicycles with location choices. *Sharing Economy*. Springer, 409–434.

Chung, Hangil, Daniel Freund, David B Shmoys. 2018. Bike angels: An analysis of citi bike's incentive program. *Proceedings of the 1st ACM SIGCAS Conference on Computing and Sustainable Societies*. ACM, 5.

Crainic, Teodor Gabriel, Michel Gendreau, Pierre Dejax. 1993. Dynamic and stochastic models for the allocation of empty containers. *Operations Research* **41**(1) 102–126.

Dai, J.G., P. Shi. 2017. A two-time-scale approach to time-varying queues in hospital inpatient flow management. *Operations Research* **65**(2) 514–536.

Erera, Alan L, Juan C Morales, Martin Savelsbergh. 2009. Robust optimization for empty repositioning problems. *Operations Research* **57**(2) 468–483.

Febbraro, Angela, Nicola Sacco, Mahnam Saeednia. 2012. One-way carsharing: solving the relocation problem. *Transportation Research Record: Journal of the Transportation Research Board* **2319**(1) 113–120.

Follmer, H., A. Schied. 2002. Convex measures of risk and trading constraints. *Finance and Stochastics* **6**(4) 429–447.

Freund, Daniel, Shane G. Henderson, David B. Shmoys. 2018. Minimizing multimodular functions and allocating capacity in bike-sharing systems. *Production and Operations Management* **27**(12) 2346–2349.

Freund, Daniel, Shane G Henderson, David B Shmoys. 2019. Bike sharing. *Sharing Economy*. Springer, 435–459.

Fricker, Christine, Nicolas Gast. 2016. Incentives and redistribution in homogeneous bike-sharing systems with stations of finite capacity. *Euro Journal on Transportation and Logistics* **5**(3) 261–291.

George, David K, Cathy H Xia. 2011. Fleet-sizing and service availability for a vehicle rental system via closed queueing networks. *European Journal of Operational Research* **211**(1) 198–207.

Ghosh, Supriyo, Michael Trick, Pradeep Varakantham. 2016. Robust repositioning to counter unpredictable demand in bike sharing systems. *Proceedings of the Twenty-Fifth International Joint Conference on Artificial Intelligence*. IJCAI'16, AAAI Press, 3096–3102.

Ghosh, Supriyo, Pradeep Varakantham, Yossiri Adulyasak, Patrick Jaillet. 2017. Dynamic repositioning to reduce lost demand in bike sharing systems. *Journal of Artificial Intelligence Research* **58** 387–430.

Hall, Nicholas G., Daniel Zhuoyu Long, Jin Qi, Melvyn Sim. 2015. Managing underperformance risk in project portfolio selection. *Operations Research* **63**(3) 660–675.

He, Long, Zhenyu Hu, Meilin Zhang. 2018. Robust repositioning for vehicle sharing. *Manufacturing & Service Operations Management* .

He, Long, Ho-Yin Mak, Ying Rong. 2019. Operations management of vehicle sharing systems. *Sharing Economy*. Springer, 461–484.

Herrmann, Sascha, Frederik Schulte, Stefan Voß. 2014. Increasing acceptance of free-floating car sharing systems using smart relocation strategies: a survey based study of car2go hamburg. *International Conference on Computational Logistics*. Springer, 151–162.

Ho, Sin C, WY Szeto. 2014. Solving a static repositioning problem in bike-sharing systems using iterated tabu search. *Transportation Research Part E: Logistics and Transportation Review* **69** 180–198.

Hu, Ming. 2018. *Sharing economy: making supply meet demand*. Springer.

Jaillet, Patrick, Jin Qi, Melvyn Sim. 2016. Routing optimization under uncertainty. *Operations Research* **64**(1) 186–200.

Jian, Nanjing, Daniel Freund, Holly M Wiberg, Shane G Henderson. 2016. Simulation optimization for a large-scale bike-sharing system. *Proceedings of the 2016 Winter Simulation Conference*. IEEE Press, 602–613.

Jordan, William C, Mark A Turnquist. 1983. A stochastic, dynamic network model for railroad car distribution. *Transportation Science* **17**(2) 123–145.

Kabra, Ashish, Elena Belavina, Karan Girotra. 2018. Bike-share systems: Accessibility and availability. *Chicago Booth Research Paper* (15-04).

Kek, Alvina GH, Ruey Long Cheu, Qiang Meng, Chau Ha Fung. 2009. A decision support system for vehicle relocation operations in carsharing systems. *Transportation Research Part E: Logistics and Transportation Review* **45**(1) 149–158.

Li, Yanfeng, WY Szeto, Jiancheng Long, CS Shui. 2016. A multiple type bike repositioning problem. *Transportation Research Part B: Methodological* **90** 263–278.

Li, Yexin, Yu Zheng, Qiang Yang. 2018. Dynamic bike reposition: A spatio-temporal reinforcement learning approach. *Proceedings of the 24th ACM SIGKDD International Conference on Knowledge Discovery & Data Mining*. ACM, 1724–1733.

Liu, Junming, Leilei Sun, Weiwei Chen, Hui Xiong. 2016. Rebalancing bike sharing systems: A multi-source data smart optimization. *Proceedings of the 22nd ACM SIGKDD International Conference on Knowledge Discovery and Data Mining*. ACM, 1005–1014.

Long, Daniel Zhuoyu, Melvyn Sim, Minglong Zhou. 2019. The dao of robustness. Available at: https://ssrn.com/abstract=3478930.

Lu, Mengshi, Zhihao Chen, Siqian Shen. 2017. Optimizing the profitability and quality of service in carshare systems under demand uncertainty. *Manufacturing & Service Operations Management* **20**(2) 162–180.

Nair, Rahul, Elise Miller-Hooks. 2011. Fleet management for vehicle sharing operations. *Transportation Science* **45**(4) 524–540.

Nourinejad, Mehdi, Sirui Zhu, Sina Bahrami, Matthew J Roorda. 2015. Vehicle relocation and staff rebalancing in one-way carsharing systems. *Transportation Research Part E: Logistics and Transportation Review* **81** 98–113.

O'Mahony, Eoin, David B Shmoys. 2015. Data analysis and optimization for (citi) bike sharing. *Twenty-ninth AAAI conference on artificial intelligence*.

Pachon, Julian E, Eleftherios Iakovou, Chi Ip, Ronny Aboudi. 2003. A synthesis of tactical fleet planning models for the car rental industry. *IIE Transactions* **35**(9) 907–916.

Pavone, Marco. 2015. Autonomous mobility-on-demand systems for future urban mobility. *Autonomes Fahren*. Springer, 399–416.

Richardson, AJ, MAP Taylor. 1978. Travel time variability on commuter journeys. *High Speed Ground Transportation Journal* **12**(1).

Robinson, Lawrence W. 1990. Optimal and approximate policies in multiperiod, multilocation inventory models with transshipments. *Operations Research* **38**(2) 278–295.

Rong, Ying, Lawrence V Snyder, Yang Sun. 2010. Inventory sharing under decentralized preventive transshipments. *Naval Research Logistics* **57**(6) 540–562.

Schuijbroek, Jasper, Robert C Hampshire, W-J Van Hoeve. 2017. Inventory rebalancing and vehicle routing in bike sharing systems. *European Journal of Operational Research* **257**(3) 992–1004.

Serna, Ainhoa, Jon Kepa Gerrikagoitia, Unai Bernabe, Tomás Ruiz. 2017. A method to assess sustainable mobility for sustainable tourism: the case of the public bike systems. *Information and Communication Technologies in Tourism 2017*. Springer, 727–739.

Shu, Jia, Mabel C Chou, Qizhang Liu, Chung-Piaw Teo, I-Lin Wang. 2013. Models for effective deployment and redistribution of bicycles within public bicycle-sharing systems. *Operations Research* **61**(6) 1346–1359.

Shu, Jia, Miao Song. 2013. Dynamic container deployment: two-stage robust model, complexity, and computational results. *INFORMS Journal on Computing* **26**(1) 135–149.

Shui, CS, WY Szeto. 2018. Dynamic green bike repositioning problem–a hybrid rolling horizon artificial bee colony algorithm approach. *Transportation Research Part D: Transport and Environment* **60** 119–136.

Simon, H. A. 1959. Theories of decision-making in economics and behavioral science. *The American Economic Review* **49**(3) 253–283.

Srinivasan, Karthik K, AA Prakash, Ravi Seshadri. 2014. Finding most reliable paths on networks with correlated and shifted log–normal travel times. *Transportation Research Part B: Methodological* **66** 110–128.

Tagaras, George. 1989. Effects of pooling on the optimization and service levels of two-location inventory systems. *IIE Transactions* **21**(3) 250–257.

The Economist. 2011. Why a boris bike can be an existential hell. URL https://www.economist.com/gulliver/2011/04/19/why-a-boris-bike-can-be-an-existential-hell.

Xie, Jingui, Gar Goei Loke, Melvyn Sim, Lam Shao Wei. 2017. The analytics of bed shortages: Coherent metric, prediction and optimization. Available at SSRN: https://ssrn.com/abstract=3041878.

Appendix A: Proof of all propositions and theorems

Proof of Proposition 2

The proof is straightforward:

$$\begin{aligned}
&\phi_\alpha\Big(\sum_{(i,j)\in\mathcal{A}}\sum_{t\in[T]}\tilde{\lambda}_{i,j}^t\eta-\sum_{(i,j)\in\mathcal{A}}\sum_{t\in[T]}y_{i,j}^{t,0}\Big)\\
=&\sum_{(i,j)\in\mathcal{A}}\sum_{t\in[T]}\alpha\log\mathbb{E}_{\hat{\mathbb{P}}}\left[\exp\left((\tilde{\lambda}_{i,j}^t\eta-y_{i,j}^{t,0})/\alpha\right)\right]\\
=&\sum_{(i,j)\in\mathcal{A}}\sum_{t\in[T]}\alpha\log\mathbb{E}_{\hat{\mathbb{P}}}\left[\exp\left(\tilde{\lambda}_{i,j}^t\eta/\alpha\right)\right]-\sum_{(i,j)\in\mathcal{A}}\sum_{t\in[T]}\alpha\log\mathbb{E}_{\hat{\mathbb{P}}}\left[\exp\left(y_{i,j}^{t,0}/\alpha\right)\right]\\
=&\sum_{(i,j)\in\mathcal{A}}\sum_{t\in[T]}\phi_\alpha\left(\tilde{\lambda}_{i,j}^t\eta\right)-\sum_{(i,j)\in\mathcal{A}}\sum_{t\in[T]}y_{i,j}^{t,0}.\quad\square
\end{aligned}$$

Proof of Proposition 3

First, it is not hard to see that $\phi_\alpha(\cdot)$ is translation invariant, i.e.,

$$\phi_\alpha(\tilde{x}_i^t-\Delta_i^t)=\phi_\alpha(\tilde{x}_i^t)-\Delta_i^t.$$

Therefore, we just need to focus on $\phi_\alpha(\tilde{x}_i^t)$. For each $i\in[N]$ and $t\in[2;T]$, we have

$$\begin{aligned}
&\phi_\alpha\left(\tilde{x}_i^t\right)\\
=&x_i^1-\sum_{j:(i,j)\in\mathcal{A}}\sum_{\tau=1}^{t-1}(y_{i,j}^{\tau,0}+z_{i,j}^{\tau,0})+\sum_{j:(j,i)\in\mathcal{A}}\phi_\alpha\left(\sum_{\tau=1}^{t-1}\sum_{s=0}^{S}\left(\mathrm{Bin}(\tilde{y}_{j,i}^{\tau,s},h_{j,i}^{\tau,s})+\mathrm{Bin}(\tilde{z}_{j,i}^{\tau,s},d_{j,i}^{\tau,s})\right)\right)\\
=&x_i^1-\sum_{j:(i,j)\in\mathcal{A}}\sum_{\tau=1}^{t-1}(y_{i,j}^{\tau,0}+z_{i,j}^{\tau,0})+\sum_{j:(j,i)\in\mathcal{A}}\phi_\alpha\left(\sum_{\tau=1}^{t-1}\sum_{s=0}^{\tau-1}\mathrm{Bin}(y_{j,i}^{\tau-s,0},\hat{h}_{j,i}^{\tau,s})\right)+\sum_{j:(j,i)\in\mathcal{A}}\phi_\alpha\left(\sum_{\tau=1}^{t-1}\sum_{s=0}^{\tau-1}\mathrm{Bin}(z_{j,i}^{\tau-s,0},\hat{d}_{j,i}^{\tau,s})\right)\\
&+\sum_{j:(j,i)\in\mathcal{A}}\phi_\alpha\left(\sum_{\tau=1}^{t-1}\sum_{s=\tau}^{S}\mathrm{Bin}(y_{j,i}^{1,s-\tau+1},\check{h}_{j,i}^{\tau,s})\right)+\sum_{j:(j,i)\in\mathcal{A}}\phi_\alpha\left(\sum_{\tau=1}^{t-1}\sum_{s=\tau}^{S}\mathrm{Bin}(z_{j,i}^{1,s-\tau+1},\check{d}_{j,i}^{\tau,s})\right)
\end{aligned}$$

where, for $(j,i)\in\mathcal{A}$,

$$\begin{aligned}
\hat{h}_{j,i}^{\tau,s}&=h_{j,i}^{\tau,s}\prod_{u=1}^{s}(1-h_{j,i}^{\tau-u,s-u}),\quad\forall\tau\in[t-1],s\in[0;\tau-1],\\
\check{h}_{j,i}^{\tau,s}&=h_{j,i}^{\tau,s}\prod_{u=1}^{\tau-1}(1-h_{j,i}^{\tau-u,s-u}),\quad\forall\tau\in[t-1],s\in[\tau;S],\\
\hat{d}_{j,i}^{\tau,s}&=d_{j,i}^{\tau,s}\prod_{u=1}^{s}(1-d_{j,i}^{\tau-u,s-u}),\quad\forall\tau\in[t-1],s\in[0;\tau-1],\\
\check{d}_{j,i}^{\tau,s}&=d_{j,i}^{\tau,s}\prod_{u=1}^{\tau-1}(1-d_{j,i}^{\tau-u,s-u}),\quad\forall\tau\in[t-1],s\in[\tau;S].
\end{aligned}$$

Now, we focus on the term

$$\phi_\alpha\left(\sum_{\tau=1}^{t-1}\sum_{s=0}^{\tau-1}\text{Bin}(y_{j,i}^{\tau-s,0},\hat{h}_{j,i}^{\tau,s})\right).$$

Notice that the summation inside ϕ function is not a summation of independent random variables; therefore, we cannot take the summation out. With a change of variable, we can get:

$$\begin{aligned}
&\phi_\alpha\left(\sum_{\tau=1}^{t-1}\sum_{s=0}^{\tau-1}\text{Bin}(y_{j,i}^{\tau-s,0},\hat{h}_{j,i}^{\tau,s})\right)\\
=&\,\phi_\alpha\left(\sum_{\tau=1}^{t-1}\sum_{\tau'=\tau}^{t-1}\text{Bin}(y_{j,i}^{\tau,0},\hat{h}_{j,i}^{\tau',\tau'-\tau})\right)\\
=&\sum_{\tau=1}^{t-1}\phi_\alpha\left(\sum_{\tau'=\tau}^{t-1}\text{Bin}(y_{j,i}^{\tau,0},\hat{h}_{j,i}^{\tau',\tau'-\tau})\right)
\end{aligned}\tag{19}$$

The last equality follows because $\sum_{\tau'=\tau}^{t-1}\text{Bin}(y_{j,i}^{\tau,0},\hat{h}_{j,i}^{\tau',\tau'-\tau})$ is independent over τ. Now, we write the binomial random variable more explicitly as:

$$\text{Bin}(y_{j,i}^{\tau,0},\hat{h}_{j,i}^{\tau',\tau'-\tau})=\sum_{i=1}^{y_{j,i}^{\tau,0}}\mathbb{1}\left(\text{Rental trip } i \text{ starts at } \tau \text{ and completes at } \tau'+1\right).$$

Therefore, Equation (19) can be further reduced to:

$$\begin{aligned}
&\sum_{\tau=1}^{t-1}\phi_\alpha\left(\sum_{\tau'=\tau}^{t-1}\text{Bin}(y_{j,i}^{\tau,0},\hat{h}_{j,i}^{\tau',\tau'-\tau})\right)\\
=&\sum_{\tau=1}^{t-1}\sum_{i=1}^{y_{j,i}^{\tau,0}}\phi_\alpha\left(\sum_{\tau'=\tau}^{t-1}\mathbb{1}\left(\text{Rental trip } i \text{ starts at } \tau \text{ and completes at } \tau'+1\right)\right)\\
=&\sum_{\tau=1}^{t-1}y_{j,i}^{\tau,0}\phi_\alpha\left(\sum_{\tau'=\tau}^{t-1}\mathbb{1}\left(\text{Rental trip } i \text{ starts at } \tau \text{ and completes at } \tau'+1\right)\right)\\
=&\sum_{\tau=1}^{t-1}y_{j,i}^{\tau,0}\delta_{j,i}^{\tau,t},
\end{aligned}\tag{20}$$

where $\delta_{j,i}^{\tau,t}$ is a constant defined as:

$$\delta_{j,i}^{\tau,t}=\alpha\log\left(1-\sum_{\tau'=\tau}^{t-1}\hat{h}^{\tau',\tau'-\tau}+\sum_{\tau'=\tau}^{t-1}\hat{h}^{\tau',\tau'-\tau}\exp(1/\alpha)\right),\quad\forall(j,i)\in\mathcal{A},t\in[T],\tau\in[t-1].$$

Similarly, we have:

$$\phi_\alpha\left(\sum_{\tau=1}^{t-1}\sum_{s=0}^{\tau-1}\text{Bin}(z_{j,i}^{\tau-s,0},\hat{d}_{j,i}^{\tau,s})\right)=\sum_{\tau=1}^{t-1}z_{j,i}^{\tau,0}\beta_{j,i}^{\tau,t},$$

where $\beta_{j,i}^{\tau,t}$ is a constant defined as:

$$\beta_{j,i}^{\tau,t}=\alpha\log\left(1-\sum_{\tau'=\tau}^{t-1}\hat{d}^{\tau',\tau'-\tau}+\sum_{\tau'=\tau}^{t-1}\hat{d}^{\tau',\tau'-\tau}\exp(1/\alpha)\right),\quad\forall(j,i)\in\mathcal{A},t\in[T],\tau\in[t-1].$$

Then, we focus on the term

$$\phi_\alpha\left(\sum_{\tau=1}^{t-1}\sum_{s=\tau}^{S}\text{Bin}(y_{j,i}^{1,s-\tau+1},\check{h}_{j,i}^{\tau,s})\right).$$

With a change of variable and then the same arguments as above, we get:

$$\begin{aligned}
&\phi_\alpha\left(\sum_{\tau=1}^{t-1}\sum_{s=\tau}^{S}\text{Bin}(y_{j,i}^{1,s-\tau+1},\check{h}_{j,i}^{\tau,s})\right)\\
=&\phi_\alpha\left(\sum_{\tau=0}^{S-1}\sum_{s=1}^{\min\{t-1,S-\tau\}}\text{Bin}(y_{j,i}^{1,\tau+1},\check{h}_{j,i}^{s,\tau+s})\right)\\
=&\sum_{\tau=0}^{S-1}\phi_\alpha\left(\sum_{s=1}^{\min\{t-1,S-\tau\}}\text{Bin}(y_{j,i}^{1,\tau+1},\check{h}_{j,i}^{s,\tau+s})\right)\\
=&\sum_{\tau=0}^{S-1}y_{j,i}^{1,\tau+1}\omega_{j,i}^{\tau,t},
\end{aligned}$$

where $\omega_{j,i}^{\tau,t}$ is a constant defined as:

$$\omega_{j,i}^{\tau,t}=\alpha\log\left(1-\sum_{s=1}^{\min\{t-1,S-\tau\}}\check{h}^{s,\tau+s}+\sum_{s=1}^{\min\{t-1,S-\tau\}}\check{h}^{s,\tau+s}\exp(1/\alpha)\right),\quad\forall(j,i)\in\mathcal{A},t\in[T],\tau\in[0;S-1].$$

Similarly, we have:

$$\phi_\alpha\left(\sum_{\tau=1}^{t-1}\sum_{s=\tau}^{S}\text{Bin}(z_{j,i}^{1,s-\tau+1},\check{d}_{j,i}^{\tau,s})\right)=\sum_{\tau=0}^{S-1}z_{j,i}^{1,\tau+1}\kappa_{j,i}^{\tau,t},$$

where $\kappa_{j,i}^{\tau,t}$ is a constant defined as:

$$\kappa_{j,i}^{\tau,t}=\alpha\log\left(1-\sum_{s=1}^{\min\{t-1,S-\tau\}}\check{d}^{s,\tau+s}+\sum_{s=1}^{\min\{t-1,S-\tau\}}\check{d}^{s,\tau+s}\exp(1/\alpha)\right),\quad\forall(j,i)\in\mathcal{A},t\in[T],\tau\in[0;S-1].$$

Combining all above results, we get:

$$\begin{aligned}
&\phi_\alpha(\tilde{x}_i^t)\\
=&x_i^1-\sum_{j:(i,j)\in\mathcal{A}}\sum_{\tau=1}^{t-1}(y_{i,j}^{\tau,0}+z_{i,j}^{\tau,0})+\sum_{j:(j,i)\in\mathcal{A}}\phi_\alpha\left(\sum_{\tau=1}^{t-1}\sum_{s=0}^{\tau-1}\text{Bin}(y_{j,i}^{\tau-s,0},\hat{h}_{j,i}^{\tau,s})\right)+\sum_{j:(j,i)\in\mathcal{A}}\phi_\alpha\left(\sum_{\tau=1}^{t-1}\sum_{s=0}^{\tau-1}\text{Bin}(z_{j,i}^{\tau-s,0},\hat{d}_{j,i}^{\tau,s})\right)\\
&+\sum_{j:(j,i)\in\mathcal{A}}\phi_\alpha\left(\sum_{\tau=1}^{t-1}\sum_{s=\tau}^{S}\text{Bin}(y_{j,i}^{1,s-\tau+1},\check{h}_{j,i}^{\tau,s})\right)+\sum_{j:(j,i)\in\mathcal{A}}\phi_\alpha\left(\sum_{\tau=1}^{t-1}\sum_{s=\tau}^{S}\text{Bin}(z_{j,i}^{1,s-\tau+1},\check{d}_{j,i}^{\tau,s})\right)\\
=&x_i^1-\sum_{j:(i,j)\in\mathcal{A}}\sum_{\tau=1}^{t-1}(y_{i,j}^{\tau,0}+z_{i,j}^{\tau,0})+\sum_{j:(j,i)\in\mathcal{A}}\sum_{\tau=1}^{t-1}y_{j,i}^{\tau,0}\delta_{j,i}^{\tau,t}+\sum_{j:(j,i)\in\mathcal{A}}\sum_{\tau=1}^{t-1}z_{j,i}^{\tau,0}\beta_{j,i}^{\tau,t}+\sum_{j:(j,i)\in\mathcal{A}}\sum_{\tau=0}^{S-1}y_{j,i}^{1,\tau+1}\omega_{j,i}^{\tau,t}\\
&+\sum_{j:(j,i)\in\mathcal{A}}\sum_{\tau=0}^{S-1}z_{j,i}^{1,\tau+1}\kappa_{j,i}^{\tau,t}.
\end{aligned}$$

□

Proof of Proposition 4

First, notice that

$$\phi_\alpha\Big(\sum_{j:(i,j)\in\mathcal{A}}(y_{i,j}^{t,0}+z_{i,j}^{t,0})-\tilde{x}_i^t\Big)=\phi_\alpha\Big(-\tilde{x}_i^{t+1}\Big).$$

Then, the final result follows by the proof of Proposition 3, and the constants are defined as:

$$\begin{aligned}
\bar{\delta}_{j,i}^{\tau,t}&=\alpha\log\left(1-\sum_{\tau'=\tau}^{t-1}\hat{h}^{\tau',\tau'-\tau}+\sum_{\tau'=\tau}^{t-1}\hat{h}^{\tau',\tau'-\tau}\exp(-1/\alpha)\right)\\
\bar{\beta}_{j,i}^{\tau,t}&=\alpha\log\left(1-\sum_{\tau'=\tau}^{t-1}\hat{d}^{\tau',\tau'-\tau}+\sum_{\tau'=\tau}^{t-1}\hat{d}^{\tau',\tau'-\tau}\exp(-1/\alpha)\right)\\
\bar{\omega}_{j,i}^{\tau,t}&=\alpha\log\left(1-\sum_{s=1}^{t-1}\check{h}^{\tau+s,s}+\sum_{s=1}^{t-1}\check{h}^{\tau+s,s}\exp(-1/\alpha)\right)\\
\bar{\kappa}_{j,i}^{\tau,t}&=\alpha\log\left(1-\sum_{s=1}^{t-1}\check{d}^{\tau+s,s}+\sum_{s=1}^{t-1}\check{d}^{\tau+s,s}\exp(-1/\alpha)\right).\quad\square
\end{aligned}$$

Appendix B: The fluid-based optimization model in Braverman et al. (2019)

Suppose that customers arrive to location i according to a Poisson process with rate $M\lambda_i$. Denote $P_{i,j}$ as the probability that a customer arrives to location i and travels to location j if there is any available vehicle at the location. Also let the travel time from location i to j to be i.i.d. exponential random variable with mean $1/\mu_{i,j}$. All other parameters are consistent with our definition in Table 2. Braverman et al. (2019) propose the following fluid-based optimization model to address the vehicle repositioning problem.

$$\begin{aligned}
\max\ &\frac{\sum_{i=1}^r a_i\lambda_i}{\sum_{i=1}^N\lambda_i}\\
s.t.\ \ &\lambda_i P_{i,j}a_i=\mu_{i,j}f_{i,j} && 1\le i,j\le N;\\
&\mu_{i,j}e_{i,j}\le\textstyle\sum_{k=1}^N\mu_{k,i}f_{k,i} && 1\le i,j\le N, j\ne i;\\
&\displaystyle\sum_{k=1,k\ne i}^N\mu_{k,i}e_{k,i}\le\lambda_i a_i\le\sum_{k=1,k\ne i}^N\mu_{k,i}e_{k,i}+\sum_{k=1}^N\mu_{k,i}f_{k,i} && 1\le i\le N;\\
&\lambda_i a_i+\displaystyle\sum_{j=1,j\ne i}^N\mu_{i,j}e_{i,j}=\sum_{k=1,k\ne i}^N\mu_{k,i}e_{k,i}+\sum_{k=1}^N\mu_{k,i}f_{k,i} && 1\le i\le N;\\
&(e,f)\in\mathcal{T}\\
&0\le a_i\le 1 && 1\le i\le N;
\end{aligned}\tag{21}$$

where the set $\mathcal{T}$ is

$$\mathcal{T}=\{(e,f)\in[0,1]^{N\times N}\times[0,1]^{N\times N}:\sum_{i=1}^N\sum_{j=1}^N(e_{i,j}+f_{i,j})=1\}.$$

Suppose $(\boldsymbol{e}^*, \boldsymbol{f}^*, \boldsymbol{a}^*)$ is the optimal solution to the fluid-based model, then according to Lemma 2 in Braverman et al. (2019), we need to adjust the solution by following procedure:

- If $a_i^* < 1$ for all $1 \le i \le N$, no need to adjust.
- Otherwise, choose any $i^{'}$ such that $a_{i^{'}}^* = 1$, define $\bar{\boldsymbol{e}}$ by letting $\bar{e}_{i,j} = e_{i,j}^*$ for all $1 \le i \ne j \le N$,

$$\bar{e}_{i^{'}i^{'}} = \sum_{i=1}^{N} e_{i,j}^*, \text{ and } \bar{e}_{i,i} = 0, i \ne i^{'}.$$

- Replace $\boldsymbol{e}^*$ with $\bar{\boldsymbol{e}}$.

Now the probability of a vehicle in location i is repositioned to location j with probability $q_{i,j}$ determined as

$$q_{i,j} = \frac{\mu_{i,j} e_{i,j}^*}{\sum_{k=1}^{N} \mu_{k,i} f_{k,i}^*}, 1 \le i \ne j \le N;$$
$$q_{i,j} = \frac{\lambda_i a_i^* - \sum_{k=1, k\ne i}^{N} \mu_{k,i} e_{k,i}^*}{\sum_{k=1}^{N} \mu_{k,i} f_{k,i}^*}, 1 \le i \le N.$$